

HU ISSN 1785-6892 in print
HU ISSN 2064-7522 online

DESIGN OF MACHINES AND STRUCTURES

A Publication of the University of Miskolc

Volume 6, Number 1 (2016)



Miskolc University Press
2016

EDITORIAL BOARD

- Á. DÖBRÖCZÖNI
Editor in Chief
Institute of Machine and Product Design
University of Miskolc
H-3515 Miskolc-Egyetemváros, Hungary
machda@uni-miskolc.hu
- Á. TAKÁCS
Assistant Editor
Institute of Machine and Product Design
University of Miskolc
H-3515 Miskolc-Egyetemváros, Hungary
takacs.agnes@uni-miskolc.hu
- R. CERMAK
Department of Machine Design
University of West Bohemia
Univerzitní 8, 30614 Plzen Czech Republic
rcermak@kks.zcu.cz
- B. M. SHCHOKIN
Consultant at Magna International Toronto
borys.shchokin@sympatico.ca
- W. EICHLSEDER
Institut für Allgemeinen Maschinenbau
Montanuniversität Leoben,
Franz-Josef Str. 18, 8700 Leoben, Österreich
wilfrid.eichlseder@notes.unileoben.ac.at
- S. VAJNA
Institut für Maschinenkonstruktion,
Otto-von-Guericke-Universität Magdeburg,
Universität Platz 2, 39106 Magdeburg, Deutschland
vajna@mb.uni-magdeburg.de
- P. HORÁK
Department of Machine and Product Design
Budapest University of Technology and Economics
horak.peter@gt3.bme.hu
H-1111 Budapest, Műegyetem rkp. 9.
MG. ép. I. em. 5.
- K. JÁRMAI
Institute of Materials Handling and Logistics
University of Miskolc
H-3515 Miskolc-Egyetemváros, Hungary
altjar@uni-miskolc.hu
- L. KAMONDI
Institute of Machine and Product Design
University of Miskolc
H-3515 Miskolc-Egyetemváros, Hungary
machkl@uni-miskolc.hu
- GY. PATKÓ
Department of Machine Tools
University of Miskolc
H-3515 Miskolc-Egyetemváros, Hungary
patko@uni-miskolc.hu
- J. PÉTER
Institute of Machine and Product Design
University of Miskolc
H-3515 Miskolc-Egyetemváros, Hungary
machpj@uni-miskolc.hu

CONTENTS

<i>Bergmann, Philipp –Grün, Florian –Gódor, István–Herbst, Klaus:</i> Methodology development for numerical evaluation of wear in tribological contacts.....	5
<i>Matisz, Norbert–Bihari, Zoltán:</i> Acoustic investigation of vacuum cleaners	15
<i>Gatzky, Thomas:</i> Industrial design in engineering programs: About the success of an integrated degree program model	21
<i>Kiss, Róbert–Takács, György:</i> Examination of suitable methods for describing machine tool structures	39
<i>Moder, Jakob–Grün, Florian:</i> Contact models for mixed friction simulation	48
<i>Szabó, Ferenc János:</i> Journal bearing optimization for minimum lubricant viscosity	56
<i>Szilágyi, Attila–Takács, György–Kiss, Dániel–Tóth, Dániel:</i> Theoretical vibration analysis of a manufacturing device	63

METHODOLOGY DEVELOPMENT FOR NUMERICAL EVALUATION OF WEAR IN TRIBOLOGICAL CONTACTS

PHILIPP BERGMANN¹–FLORIAN GRÜN²–ISTVÁN GÓDOR³–
KLAUS HERBST⁴

^{1, 2, 3}*Chair of Mechanical Engineering, Montanuniversität Leoben,
philipp.bergmann@unileoben.ac.at*

⁴*Miba Gleitlager GmbH, klaus.herbst@miba.com*

Abstract: Hydrodynamic journal bearings in internal combustion engines suffer progressively from hindered operation conditions. Consequently the chance of wear and failure increases making wear prediction and simulation inevitable. For the purpose of numerical wear evaluation we implemented a modified Archard's wear law in COMSOL Multiphysics® and applied it on a test rig. Necessary wear coefficients were determined based on close-to-component tribological wear tests. By comparing numerical and achieved test results the usability of the developed methodology was evaluated. Results reveal the suitability to assess wear locally and chronologically resolved.

Keywords: *Tribology, Journal bearing, Simulation, Wear assessment*

1. INTRODUCTION

Due to actual legislative regulations for automotive industry implying a cap of average 95 g CO₂/km for an OEM's fleet by 2020 an overall increase of vehicles' efficiency is necessary. Areas which can contribute significantly to this ambitious goal are among others light weight design, downsizing, the reduction of frictional losses and hybridization. Looking onto the topic of hydrodynamic journal bearings in internal combustion engines (ICE) in this context, performed actions lead to higher specific loads and imply hindered conditions. As a consequence the chance of wear and failure increases which needs to be taken into account in a machines design by numerical wear assessments. One of the most prominent wear models goes back to Archard [1]. Based on material parameters and an empirical coefficient this model allows a numerical implementation in the multiphysics simulation software COMSOL Multiphysics® [2], [3].

In the following journal bearings' characteristics as well as the impact of actual developments on journal bearings is described with the help of Stribeck-curves. The tribological test methodology developed at the Chair of Mechanical Engineering to calculate necessary wear coefficients of arbitrary material combinations by using a rotary tribometer TE92HS from Plint Phoenix Tribology in combination with a journal bearing adapter (JBA) follows this first part. The setting of the numerical model of the JBA is described and finally numerical and test results are compared.

2. JOURNAL BEARINGS – SETUP AND FUNCTIONALITY

Journal bearings typically comprise of a steel shaft, a softer multilayer journal bearing shell and the lubricant, see *Figure 1*. The relative motion of the shaft and journal bearing results in a fluid film gap geometry allowing a hydrodynamic pressure build up which is in equilibrium with an external load F_{ext} . Dependent on load, rotational speed and temperature the operation point of a journal bearing varies. A Stribeck-curve visualizes this circumstance by plotting the coefficient of friction COF or μ against the Hersey number or in most cases against the relative speed, see *Figure 2*; full line. With increasing Hersey number frictional behaviour changes from solid friction to boundary and mixed friction. During these regimes of friction the surfaces are in contact leading to high frictional losses and wear. After the release point the mating surfaces are separated and the system's behaviour changes to fluid friction in which the conventional area of operation is situated. Increasing shear forces lead to a rise of frictional losses in this regime.

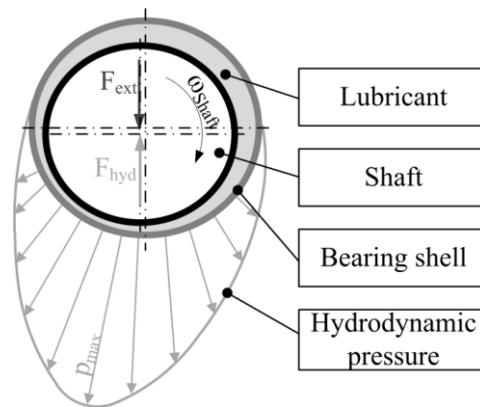


Figure 1. Principle set up of a journal bearing comprising of a shaft, a bearing shell and a lubricant in between separating both surfaces by hydrodynamic pressure

The intensity of wear is tight-knit to the occurring friction regimes. While solid, boundary and mixed friction regimes generally lead to high wear, wear in fluid friction regime is comparable low [4]. The impact of actual developments including light weight design, downsizing, the reduction of frictional losses and hybridization on the frictional behaviour of journal bearings can be visualized descriptive with help of Stribeck-curves in *Figure 2*. To reduce fluid frictional losses in the conventional area of operation the usage of low and ultra-low viscosity oils is contemplated resulting in lower fluid film thicknesses which widen the area of boundary and mixed friction towards higher rotational speeds [5]. The same line take higher specific loads resulting from downsizing and light weight design.

Additionally the upcoming start/stop technology leads to a frequent run through the already widened areas of boundary and mixed friction making wear in journal bearings to a delicate topic [6], [7].

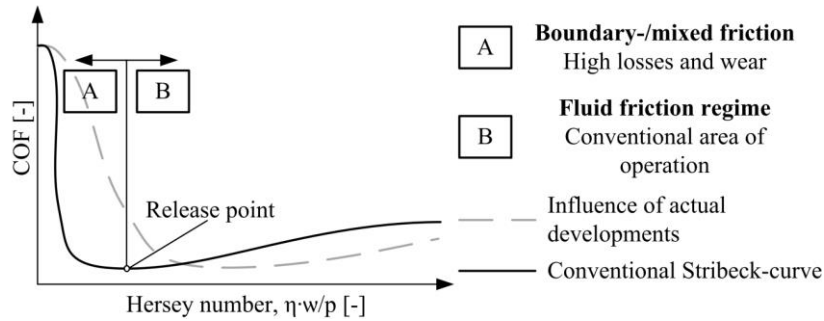


Figure 2. The full line represents a conventional Stribeck-curve. The impact of actual developments is depicted by the dashed line

3. NUMERICAL INCORPORATION OF WEAR LAWS

Wear models link a resulting wear quantity, e.g. wear height or wear volume to the properties of the mating materials and information about the contact state and duration. Archard's law, see equation 1, is widely used and links the worn volume W to the normal force P , the sliding distance s , the flow pressure of the softer material p_m and an empirical material-related constant K , which describes the probability to produce a wear particle [1].

$$W = \frac{K \cdot s \cdot P}{p_m} \quad (1)$$

This wear equation can be incorporated in COMSOL Multiphysics[®] after some mathematical manipulation by defining an ordinary differential equation (ODE), see Equation 2. The material dependent variables K and p_m are combined to the wear intensity C , which describes the dependence of wear volume on frictional energy as a result of solid contact in relative motion. This parameter can be derived from test data. By differentiating equation (1) with respect to time and identifying $\partial s / \partial t$ as the sliding velocity v of the counterpart surface and p as the normal solid contact pressure acting on the surface, the necessary ODE can be deduced.

$$\frac{\partial w}{\partial t} = C \cdot p \cdot v \quad (2)$$

4. TEST METHODOLOGY

Tests to achieve the necessary wear intensities were conducted on a rotary tribometer TE92HS from Plint Phoenix Tribology mainly comprising of a motor (I), the shaft (II) and the journal bearing adapter (JBA) (III). The specific set up can be found in [8]. The adapter realizes the tribological system of a real life journal bearing shell and a shaft specimen in an oil bath, which contains the lubricant and can be heated.

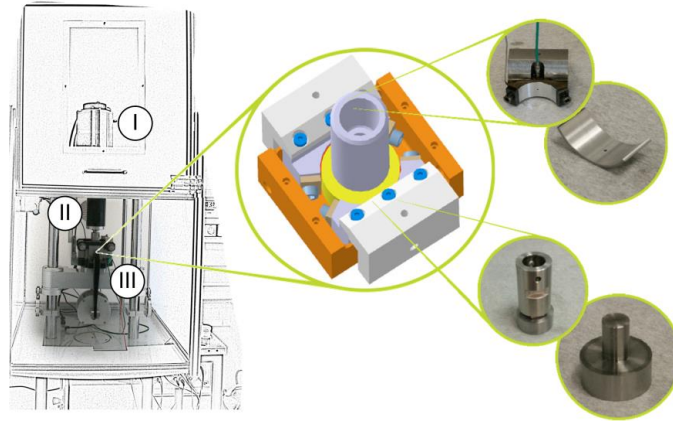


Figure 3. Test set up of the rotary tribometer TE92HS and the journal bearing adapter (JBA)

The input parameters are load p , the system's temperature T_1 and rotational speed n . The system's behaviour can be described using the coefficient of friction (COF), the contact potential (CP) and the close to contact temperature T_2 . The CP sheds light on the state of contact, whereby a CP-value of 0 mV states direct contact of bearing shell and shaft specimen. A rising CP-suggests an increasing separation of the solid surfaces until complete separation of both surfaces by a lubrication film. Additional measurements, in particular the contact close temperature T_2 and the hydrodynamic pressure allow more insights of the occurring tribological processes [7]. Figure 4 shows an exemplary graph of a Stribeck-curve and how available measurement data can explain the tribological processes.

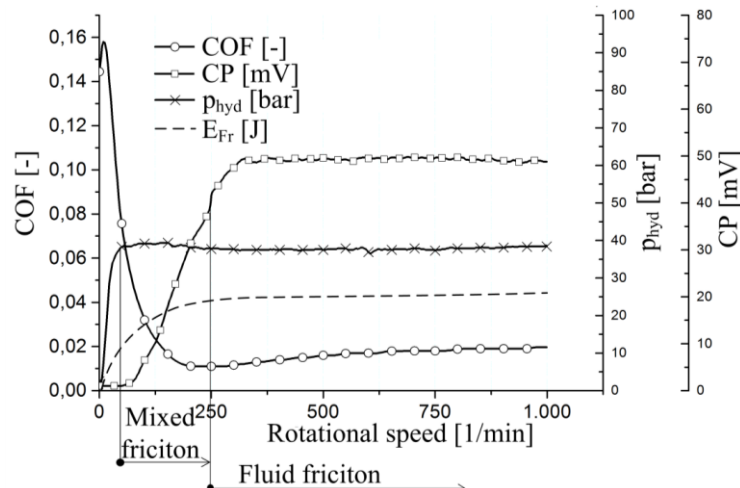


Figure 4. Exemplary Stribeck-curve

Starting from zero rotational speed the COF sinks with increasing speed. Simultaneously the contact potential CP as well as the hydrodynamic pressure p_{hyd} rise, showing that the load is increasingly carried by the p_{hyd} and the solid contact share reduces. After the release point at around 250 rpm the system operates in fluid friction, indicated by high CP -values and the COF which starts to rise again.

Based on the normal force F_N , the measured COF, the rotational speed n , the acquisition frequency f , the shaft specimen radius r and the CP the resulting frictional energy E_{Fr} is calculated. The CP acts as a weighting coefficient to consider the state of friction and the intensity of wear, whereby the CP_{Fluid} indicates the CP -value of the fluid friction regime:

$$E_{Fr} = F_N \cdot \mu \cdot \frac{2 \cdot \pi \cdot n \cdot r}{f} \cdot \left(1 - \frac{CP}{CP_{Fluid}}\right) \quad (3)$$

The standard data acquisition mode enables an acquisition frequency of 1 Hz. Since the start/stop cycles occur in a period of time of 5 seconds, this type of data acquisition doesn't deliver enough information. To bypass this lack of information every specified number of cycles the rising ramp is recorded with a frequency of 1 kHz. After an additional cycle the decreasing ramp is also recorded with the same frequency. This in high speed measurement recorded data is taken as representative data for the following cycles. To record wear heights and volume, the thickness of selected points over the specimens' surface as well as the weight of the bearing specimens are measured before and after the tests. The test program of conducted tests is depicted in *Figure 5*.

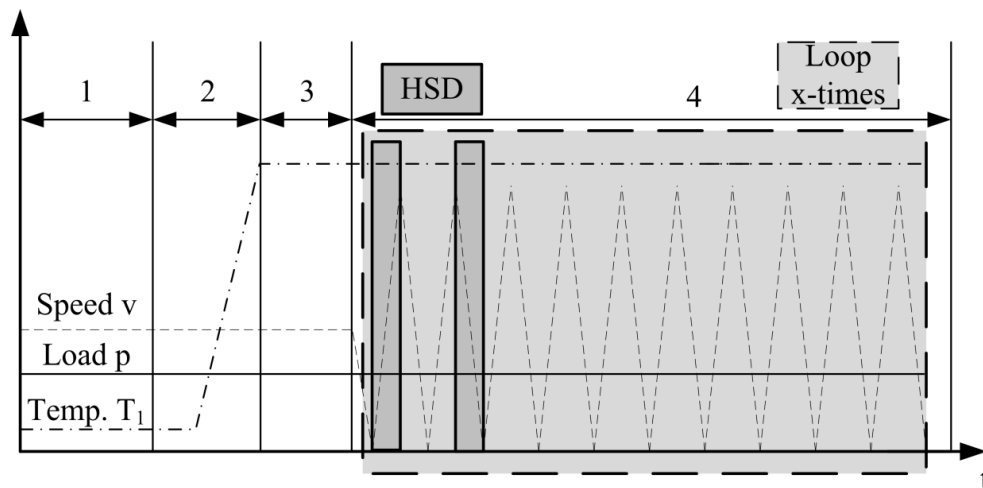


Figure 5. Schematic test program

After applying the maximum load the system is set to a moderate speed during a running in phase (1). In this step the surfaces adjust to each other leading to an energetic favourable state. In Step 2 the system is heated up to the aspired test temperature. Due to inertial thermal effects a compensation phase (3) is included. The subsequent step 4 includes a defined number of start/stop cycles. By reducing the rotational speed to zero and then starting again while keeping the other parameters constant, the tribological system runs through all regimes of friction. During this time high speed data (HSD) measurements are taken for the calculation of frictional energy. To evaluate the wear intensity tests with varying number of cycles were conducted. The material under investigation was a lead based overlay on a bronze lining and a standard crank shaft steel shaft. Shell Rimula 10 W was used as lubricant.

5. TRIBOMETRIC RESULTS

In *Figure 6* on the left hand side an exemplary test graph showing the run of the contact close temperature T_1 , the systems temperature T_2 , the COF, and normal load F_N is depicted. Due to the chronological representation the resulting Stribeck-curves reduce to single peaks. Therefore a zoom is shown on the right hand side additionally including the speed and the CP . The system operates in a steady state and wears continuously when low sliding speed leads to an insufficient hydrodynamic pressure build up resulting in solid contact, which is indicated by a breakdown of the CP .

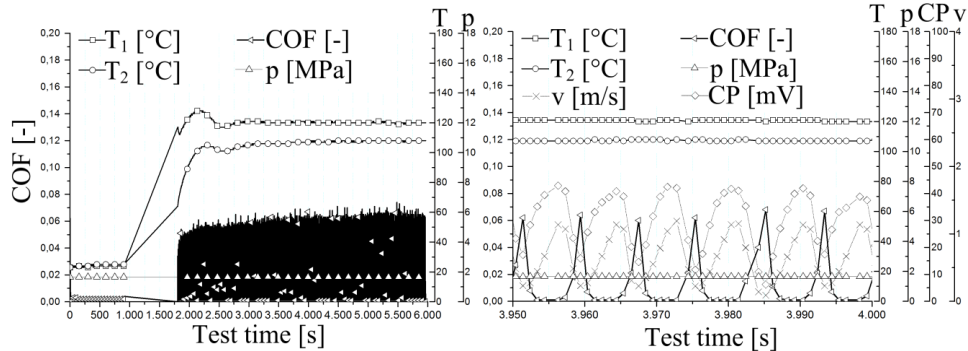


Figure 6. Left: Test plot of a start/stop wear test. Right: Zoomed period of time depicting steady state start/stop behaviour

With *Equation (3)* the frictional energetic entry can be calculated and plotted in relation to the resulting wear volume, see *Figure 7*. With increasing number of cycles and consequently increasing frictional energy the wear volume increases linearly. This characteristic is comparable to available data in literature and allows retrieving a constant wear intensity C from measured data.

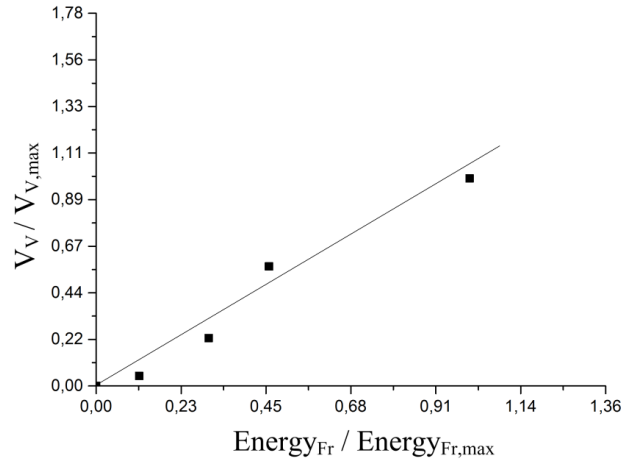


Figure 7. Wear characteristic

6. NUMERICAL MODEL SET UP

A numerical model is set up in COMSOL Multiphysics® representing one half of the JBA. The specimen adapter is loaded with a time dependent external force acting on boundary A. On the journal bearing's surface, boundary B, the Reynolds equation is solved so that the external force stays in a dynamic equilibrium with the resulting hydrodynamic pressure. Boundary C, D and E are restrained by roller conditions only allowing deformation in tangential direction. Additionally the mesh is shown in Figure 8, which was chosen rather coarse since the test functions are quadratic and no sharp gradients of the solution are expected.

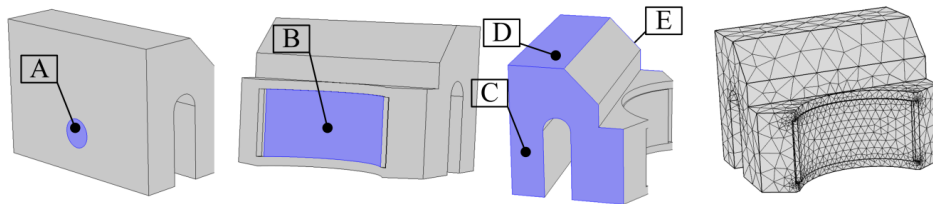


Figure 8. Numerical model set up. Boundary A: external load, boundary B: hydrodynamic load, boundary C, D and E: constraint normal deformation. The mesh is shown on the right hand side

Deformation of the JBA's structure is taken into account. The shaft specimen, however, can be considered as rigid due to its high stiffness in comparison to the bearing shell and specimen adapter. Subsequently the shaft is not modelled and only considered as shaping geometry of the fluid film. In the case of small film thicknesses surface roughness asperities interact and the surfaces come into contact. To take solid contact into account a contact model according to Greenwood

and Williamson was implemented yielding an additional pressure dependent on the fluid film thickness [9]. This statistical model can be described with equation (4) and can basically be divided in the stiffness part including geometric and material parameter (combined Young's modulus E' , asperity density n , mean asperity radius R) of the surface and a standard probability function taking the statistical distribution of the asperity heights into account. d represents the actual fluid film thickness.

$$p = \frac{4}{3} \cdot E' \cdot n \cdot \sqrt{R} \cdot \int_d^{\infty} (z - d)^{\frac{3}{2}} \Phi(z) dz \quad (4)$$

The wear law, *Equation 2*, is implemented by an ODE on the surface of the journal bearing (boundary B). For evaluation purposes of the set up numerical model a period of start/stop was taken into account with parameters taken from the test configuration: $F_N = 1500$ N; $n = 0.01$ –500 rpm; $T = 110$ °C. Since a sliding speed of 0 rpm would lead to a singularity a low rotational speed was chosen to avoid this problem.

7. RESULTS

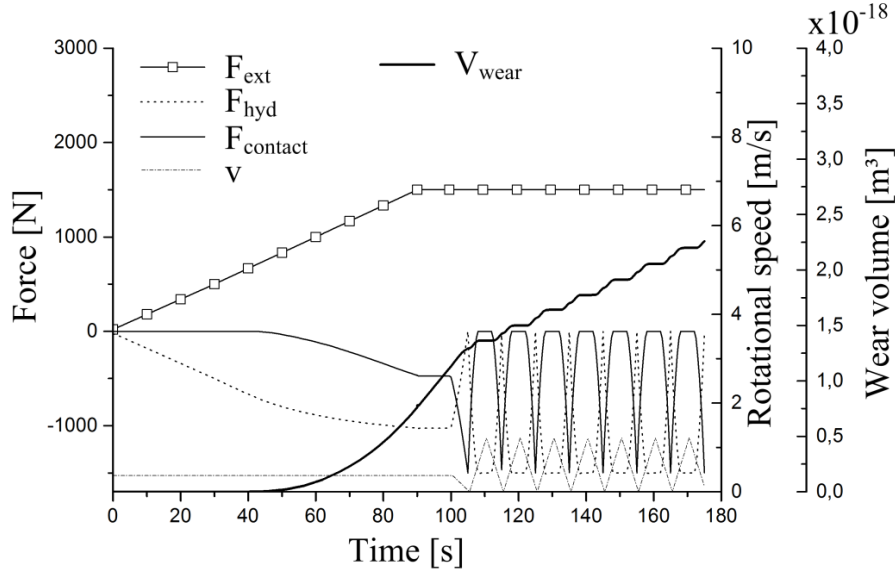


Figure 9. Resulting quantities of the numerical time dependent test sequence

Figure 9 shows the simulated run of the external load F_{ext} , which is kept constant after ramping it from an initial state, the hydrodynamic load F_{hyd} and the force resulting from solid contact $F_{contact}$. During the initial phase of loading the external force is in equilibrium with the hydrodynamic force only. When the carrying capacity of the hydrodynamic force is exceeded, meaning that the fluid film thickness drops under the roughness value of the surfaces, the solid contact force contributes

to the force equilibrium starting at approximately 40 seconds. Simultaneously process of wear starts and the wear volume rises. At 100 seconds start/stop cycles start. As a consequence of the varying rotational speed ν (0.01– 500 rpm) the hydrodynamic carrying capacity changes. The residual load share needs to be carried by solid contact. During the periods of solid contact wear volume increases while staying at a constant level when the load is carried by hydrodynamic force solely.

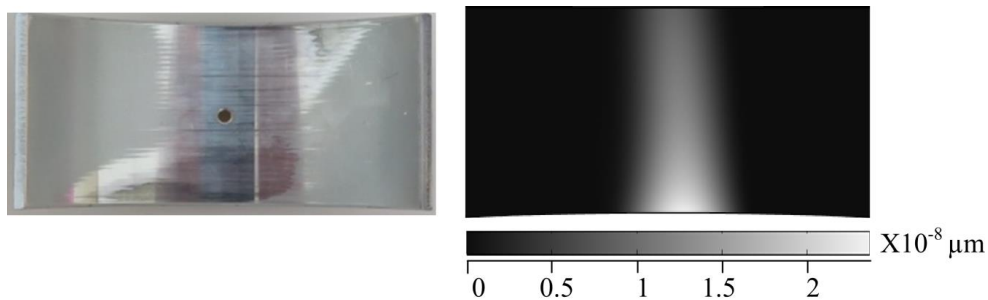


Figure 10. Comparison of contact pattern resulting from numerical investigations (left) and test specimen (right)

The simulation was stopped after 7 start/stop cycles. After the performed start/stop cycles an accumulated wear volume $2.27 \times 10^{-18} \text{ m}^3$ and a maximum wear height of $2.37 \times 10^{-8} \mu\text{m}$ arose. The methodology is evaluated by comparing the resulting wear pattern of test (left) and simulation (right), see *Figure 10*. The bearing shell exhibits an area of intense wear at the lower boundary indicated by a darker dislocation. The same holds for the simulated wear pattern.

8. SUMMARY

- A simulation methodology incorporating a time-dependent wear investigation based on the Archard wear law of the JBA was set up.
- Necessary wear coefficients wear observed by conducted tests on the JBA and consequently a strong relation to the real wear processes in numerical investigations could be incorporated.

9. CONCLUSION

- The developed methodology in COMSOL Multiphysics® represents a meaningful and fast to adapt tool to assess wear in arbitrary tribological contacts.
- The results depict a good agreement with test data qualitatively and a good suitability as a wear assessment tool for generally lubricated contacts with wear resulting from arbitrary solid contact.
- For qualitative statements it is necessary to take fluid properties into account properly, implement a suitable contact model and especially focus on retrieving significant wear coefficients.

10. ACKNOWLEDGEMENT

Financial support by the Austrian Federal Government (in particular from Bundesministerium für Verkehr, Innovation und Technologie and Bundesministerium für Wissenschaft, Forschung und Wirtschaft) represented by Österreichische Forschungsförderungsgesellschaft mbH and the Styrian and the Tyrolean Provincial Government, represented by Steirische Wirtschaftsförderungs-gesellschaft mbH and Standortagentur Tirol, within the framework of the COMET Funding Programme is gratefully acknowledged. In addition the authors are deeply grateful to the company partner Miba Gleitlager GmbH for their support.

REFERENCES

- [1] ARCHARD, J. F.–HIRST, W.: Wear of metals under unlubricated conditions. *Proceedings of the Royal society of London. Series A, Mathematical and Physical Sciences*, 1956, 397–410.
- [2] ELABBASI, N. H.–HANCOCK, M. J.–BROWN, S. B.: Simulating Wear in Disc Brakes. *COMSOL Conference 2014*, Boston.
- [3] SUTTON, D.–LIMBERT, G.–STEWART, D.–WOOD, R. J. K.: Simulation of Wear using LiveLink™ for MATLAB®. *COMSOL Conference 2013*, Rotterdam.
- [4] STACHOWIAK, G. W.–BATCHELOR, A. W.: *Engineering Tribology*. 3rd edition. Elsevier Butterworth-Heinemann, 2005.
- [5] MARTINEZ, B. T.–MARTINEZ, V. M.–ROA, L. R.–GUTIÉRREZ, T. P.: Evaluation of the Fuel Economy Improvement due to Low Viscosity Lubricants in a Light Duty Diesel Engine Running under the New European Driving Cycle (NEDC). *19th International Colloquium Tribology – Industrial and Automotive Lubrication*. Stuttgart, Germany, 2014.
- [6] SUMMER, F.: *Tribometric assessment towards functionality of current and future journal bearing systems*. Montanuniversität Leoben, Phd-thesis, 2016.
- [7] BERGMANN, P.–SUMMER, F.–GRÜN, F.–GÓDOR, I.–OFFENBECHER, M.–LAINÉ, E.: Tribological Investigations of Journal Bearings by means of a close to component Test Methodology. *ÖTG Symposium 2014*, 113–121.
- [8] GRÜN, F.–KRAMPL, H.–SCHIFFER, J.–MODER, J.–GÓDOR, I.–OFFENBECHER, M.: Tribometric Development Tools for Journal Bearings – a novel test adapter. *World Tribology Congress 2013*.
- [9] GREENWOOD, J. A.–WILLIAMSON, J. B. P.: Contact of Nominally Flat Surfaces. *Proceedings of the Royal society of London. Series A, Mathematical and Physical Sciences*, 1966, 300–319.

ACOUSTIC INVESTIGATION OF VACUUM CLEANERS

NORBERT MATISZ–ZOLTÁN BIHARI

*Institute of Machine and Product Design, University of Miskolc
H-3515 Miskolc-Egyetemváros
matisznorbi@gmail.com; machbz@uni-miskolc.hu*

Abstract: The noises evolving from our environment can be defined as pollutants, as they can lead to the impairment of different environmental factors (e.g: air, soil, waters). Within environmental noise sources we differentiate between noises caused by industry or traffic. Noises emitted during flow and the noise of machinery is considered industrial noise, which are mainly emitted during the flow of fluid for gasses. The aerodinamical noise effects (e.g.: safety valves, compressors, ventillation systems, pneumatic machinery, vacuum cleaners) which were widespread with the development of different technologies are considered to be the highest intensity noise sources [1]. In this article we focus on the investigation of the noises emitted by household machinery, specifically vacuum cleaners.

Keywords: *vacuum cleaner, noise pressure levels, Brüel & Kjaer, 3rd octave band analysis*

1. INTRODUCTION

The noises emitted by using vacuum cleaners are caused by the engine itself but mainly by the flow of the medium forming in the tube. For many people vacuum cleaning can cause a headache. This can be traced back to the noise emitted by the machine. The noise reduction of vacuum cleaners was investigated by Electrolux Ltd. among others. The Ultra Silencer type vacuum manufactured by them is considered to be really quiet as the 68 dB noise emission is even less then the noise produced by watching TV [3]. However this isn't negligible either because almost all laws define the noise emission limit at 65 dB, above this level noise can harmfully effect living organisms.

2. EXECUTION OF MEASUREMENTS

Our tests were conducted on 3 different vacuum heads provided to us by Electrolux Ltd which were operated with the Ultra Silencer vacuum cleaner. The vacuum cleaner we used was the Electrolux Vol. 1 Type, serial number: 34200852, it's maximum performance is 2200 W. The acoustical test was performed in the semi-anechoic chamber of the University of Miskolc Institute of Machine and Product Design equipped for this purpose. Our goal was to determine the vacuum heads' noise output levels on 3 different suction levels. For this – according to the “surface sheathing” method – we measured the noise pressure levels in 9 monitoring points in 1 m distance.

The vacuum cleaner itself was placed outside the chamber in order to filter out the mechanical noise emitted by the engine. Only the vacuum tube and the 3 vacuum heads were placed inside the chamber. The tube was sealed with acoustic insulation material to filter out the noise emitted by the tube.

The heads were connected to the vacuum by a 40 mm diameter PVC tube which we connected to a Prandtl-tube. We needed the Prandtl-tube to register the pressure differences inside the plastic tube with the help of a pressure metering device; from these values we can calculate the flow velocity. The suction levels used by us are the equivalents of 2,7 m/s; 4,7 m/s; 6,1 m/s; flow velocities. The noise pressure levels were measured by the Brüel & Kjær Observer 2260 type integrating noise meter and third band octave analyser. From the measured values we calculated the special averages and noise output levels according to the EN 60704 standard. The test sequence was performed on the carpet that was defined for this purpose by the standard.

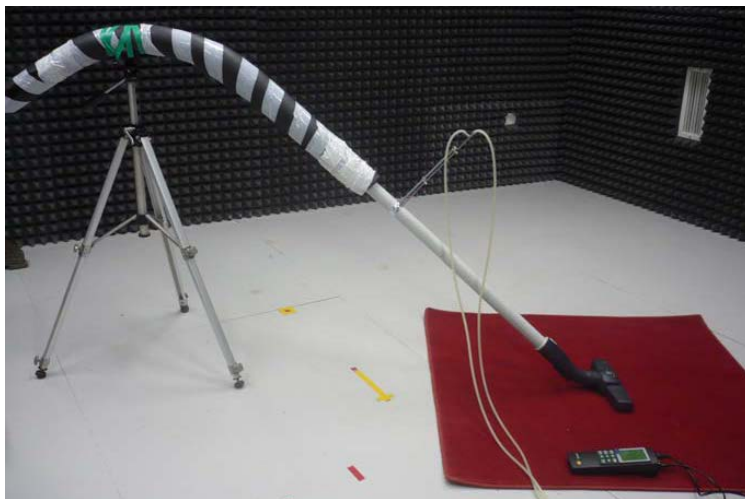





Figure 1. Placement of the equipment according to standard

Before starting the tests we calibrated the equipment and registered the meteorological conditions. The temperature was 23,9 C°; pressure was 1051,6 MPa; the relative humidity of the air was 61%. These results were provided by the equipment measuring meteorological data that were installed in the laboratory. Following the arrangement and calibration of the equipment, we measured the environmental background noise which was 17,7 dB. Because the difference of the measured value, and the background noise is more than 10 dB in every measured point we overlooked its effect during the evaluation of the tests. Following the measurement of background noise we metered the A-sound pressure levels in 15-15 second time intervals in 9 different monitoring points with the vacuum cleaner on operating warmth.

3. EVALUATION OF TEST RESULTS, CONCLUSIONS

The noise output levels calculated from the test results can be observed in the *Table 1* and *Figure 2*. both show well, that according to expectations all 3rd vacuum head's noise output levels increased with the increase of the flow velocity. In the case of the 1st vacuum head the noise output was raised with 8 dB and another 5 dB, with vacuum head 2nd the noise output level increased with 13 dB and another 4 dB, with the 3rd vacuum head the noise output increased with 12 dB, then 3 dB with the increase of the revolution number.

Table 1
Comparison of noise-output levels

Vacuum Cleaners		v [m/s]	L _w [dB]
The first cleaner head		2,7	60
		4,7	68
		6,1	73
The second cleaner head		2,7	55
		4,7	68
		6,1	72
The third cleaner head		2,7	54
		4,7	66
		6,1	69

As the figure shows the 1st vacuum head caused the highest noise-output level, while the 3rd vacuum head with the most complex geometry strains the environment the least.

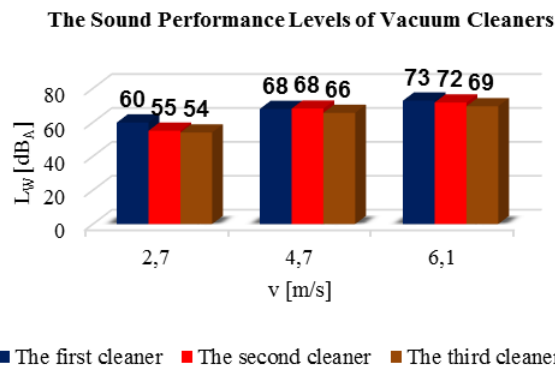


Figure 2. Noise-output levels of the vacuum heads on the carpet

From the values in *Table 1* we can see that on the lowest suction level the 1st vacuum head produced a noise-output level of 60 dB while on the highest we measured 73 dB. Therefore while we set the rev count on the vacuum cleaner from the smallest to the maximum value, the noise level increased with $\Delta L = 13$ dB in the case of the 1st vacuum head. According to the rules of the qualification of levels we relate back to the $P_0 = 10^{-12}$ W referential value, we calculate the noise-output levels:

$$P_{min} = 10^{-12} \cdot 10^{6,0} = 10^{-6} \text{ W}, \quad (1)$$

$$P_{max} = 10^{-12} \cdot 10^{7,3} = 2 \cdot 10^{-5} \text{ W}. \quad (2)$$

Relation of noise-outputs according to (1) and (2):

$$\frac{P_{max}}{P_{min}} = \frac{2 \cdot 10^{-5}}{10^{-6}} = 20. \quad (3)$$

We can conclude that with the 1st vacuum head the acoustical output was raised to an estimate 20-fold value, which is not an inconsiderable multiplier while the flow velocity “only” increased to its 2,3 times value. In case of the 2nd head the noise-output level is increased with a value of $\Delta L = 17$ dB which is a considerate, estimated 63,5 times increased value (With the 3rd head $\Delta L = 15$ dB equals to around a 32 times increased value).

4. 3RD OCTAVE BAND ANALYSIS OF THE MARK1 VACUUM HEAD

Beside focusing on the determination of the noise-output levels we executed a different test as well, its purpose was the determination of the noise-output levels per third octave band. In this case for the sake of simplicity we only had a single monitoring point on which we measured the 3 vacuum heads from a 1 m distance, and registered the noise pressure levels belonging to the 3rd octave band mid-frequencies. We operated the vacuum cleaner on maximum suction capacity on operating warmth. For this we had the machine run in idle for 15 minutes.

Before conducting the test we measured the background noise with 3rd octave band analysis. As a result we observed that the difference of the measured value, and the background noise is more than 10 dB, therefore we disregarded it. In the 3rd octave bands under 125 Hz the noise level was insignificant.

The instrument and its microphone was placed on suitable stand while securing equal measuring conditions for each vacuum head. During the course of the test we used the A-filter specified for human-centric measurements in all 3 cases.

The measured A-sound pressure levels per 1 m 3rd octave band are shown in the *Table 2*. *Figure 3* shows these values in diagram form, from which it can be clearly seen that the vacuum head marked 1st strains the environment with the most amount of noise. The difference is not significant, but from the perspective of the full sound frequency interval, the rundown of the components per 3rd octave band is

much more even in the case of the 3rd vacuum head. This is unmistakably the result of better engineering creating a better flow environment.

Table 2
Sound pressure levels of vacuum-heads by 3rd octave band metering

f _m [Hz]	L _p [dB _A]		
	The first cleaner	The second cleaner	The third cleaner
125	19,7	20,1	19,4
160	23,3	23,8	22,6
200	35,2	35,0	35,3
250	35,6	34,8	34,9
315	38,8	39,0	38,9
400	47,0	46,9	43,8
500	44,9	45,7	40,1
630	50,6	54,7	47,1
800	51,0	56,7	51,5
1000	52,0	53,4	51,3
1250	60,2	52,7	52,3
1600	56,2	54,7	51,0
2000	47,9	52,3	49,0
2500	46,5	45,1	41,7
3150	47,1	44,1	39,4
4000	43,8	37,7	35,2
5000	42,3	39,3	35,8
6300	47,6	45,7	40,5
8000	41,9	39,6	35,0
10000	33,2	27,8	28,4
12500	25,2	23,3	22,8
16000	24,1	19,2	17,5
20000	27,5	17,5	15,5
Overall	63,5	62,7	59,0

The raised section $f_m = 400$ Hz mid-frequency 3rd octave band was caused by the rotating frequency of the vacuum's rotating component. We experience the highest sound pressure level in the case of the 1st vacuum head, in the 125 Hz mid-frequency 3rd octave band (60,2 dB). In the case of the $f_m = 6300$ Hz mid-frequency 3rd octave band a significant peak can be observed. Supposedly this is caused by

the drive unit of the vacuum cleaner, namely the blade frequency of the turbine. This supposition could be cleared up with an FFT test.

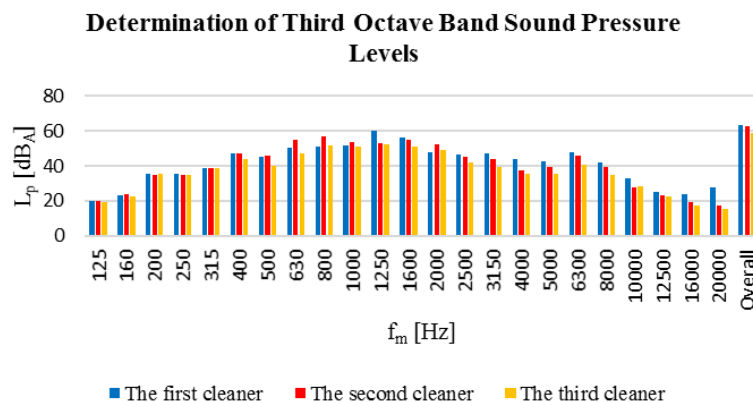


Figure 3. A-sound pressure levels per 3rd octave band of the vacuum heads (on the carpet)

Evaluating the different tests conducted on the vacuum heads we can establish a definite order considering noise emission and we can conclude that the vacuum head marked 3 with the most complex geometry strains the environment with the least amount of noise.

5. OPPORTUNITIES FOR FURTHER INVESTIGATION

So far we can only conclude these observations from the tests, however there is room to conduct further investigations. The flow simulation software called AnsyFluent has a noise module with which our further goal is to detect the flow emitted noise of the arbitrarily selected vacuum heads through simulation tests. We expect to get similar dB values to our test results.

6. ACKNOWLEDGEMENTS

This research was carried out as part of the TAMOP-4.2.1.B-10/2/KONV-2010-0001 project with support by the European Union, co-financed by the European Social Fund.

REFERENCES

- [1] BARÓTFI, I.: *Környezettechnika*. Mezőgazda Kiadó, Budapest, 2000.
- [2] BIHARI, Z.–TÓBIS, Zs.–SARKA, F.: *Akusztikai és rezgéstani minőség*. Nemzeti Tankönyvkiadó, Budapest, 2010.
- [3] <http://www.electrolux.hu/termektamogatas/Hasznos-tippek/Vacuum-cleaners/>
- [4] Brüel & Kjær: *Product Data*. <http://vip.tilb.sze.hu/avlab/2260.pdf> (letöltés ideje: 2015. 11. 08.)

INDUSTRIAL DESIGN IN ENGINEERING PROGRAMS: ABOUT THE SUCCESS OF AN INTEGRATED DEGREE PROGRAM MODEL

THOMAS GATZKY

*Prof. h.c. HD Dipl.-Formgestalter, Dipl.-Ing.
Otto-von-Guericke-University of Magdeburg
Faculty of Mechanical Engineering
Research and Teaching Area Industrial Design
thomas.gatzky@gmail.com*

Abstract: Product development is an interdisciplinary and dynamic process. Especially in its early stages, engineers and industrial designers, among others, have a substantial say in the cost-intensive decisions being prepared and made.

The Master's program in Integrated Design Engineering (IDE) is based on the Magdeburg model of integrated product development and aims at preparing future engineers to apply human-centred, integrated product development methods. It also offers opportunities to integrate industrial design into the engineering program.

Creating products for people means to design all future product characteristics in a way that helps people handle the product, eases its use, and makes it safe and emotionally attractive for the user. The industrial design curriculum focuses on analysing aesthetic and ergonomic product requirements.

Design tasks focus on the use scenario of the product to be designed and its perceptually adequate form as key challenges of the design process.

In IDE development projects, students can practice a holistic and integrated approach to designing. These projects present an ideal experimenting ground where engineers and designers learn to work together.

Keywords: *integrated product development, industrial design specialty in an engineering program, aesthetic and ergonomic product requirements, use scenario and perceptually adequate designing, Master's program in Integrated Design Engineering (IDE)*

INTRODUCTION

Product development is a dynamic, interdisciplinary process that involves cost-determining decisions, especially in the early stages, to which engineers and industrial designers contribute significantly. However, it is a well-known phenomenon that engineers and industrial designers have “difficulties” in communicating with each other. Where do these problems come from? Do they have an objective base and if so, is it possible to mitigate them or even use them productively?

This paper asks a number of hypothetical questions about ways to ease conflicts between engineers and designers. The industrial design courses within the engineering program offered at the University of Magdeburg provides some answers to how to ease potential conflicts. The overall goal, however, is to make the product development process more efficient, and for students to learn to design products according to holistic quality standards.

1. OPPORTUNITIES AND CONFLICTS – AN ATTEMPT TO DEFINE THE SITUATION

Since the 17th and 18th century, product development has increasingly become a team effort. By devising subject-specific approaches and development methods (methodological research in engineering design) and related design tools, individual specialty fields have made tremendous progress. The engineering disciplines have advanced in a co-ordinated manner in contrast to the relationship between industrial design and engineering design. Numberless attempts undertaken in the 1970s and 1980s to depict the industrial design process in much the same manner as the engineering design process were understandable but did not resonate in everyday design practice. Especially computer-aided design tools developed in different directions. The initial incompatibility of CAD and CAID programs was an expensive nuisance.

There are many reasons to explain the situation but the decisive factor is the different approach design engineers and industrial designers pursue. As shown in *Figure 1*, both approaches differ fundamentally with regard to the time the geometrical-physical and functional product design is created in its entirety.

1.1. Causes of conflict

Industrial designers and design engineers are both designers. Both disciplines aim at contributing to the development of a physical product. Both disciplines are mainly responsible for creating a geometrical-material product. Design engineering and technological requirements such as adequate load, material and production specifications have a direct impact on the embodiment of structural parts, components, sub-assemblies, and entire products.

What both disciplines have in common is designing a geometrical-physical product according to technical *and* aesthetic product specifications, but this objective also creates problems since both disciplines approach the common development objective from very different angles. Differing discipline-related goals, approaches, development methods, and design tools have led to a distinctive division of labor in the early phases of product development. The differing approaches to industrial design and engineering design, which are reasonable from a content-related perspective, have often created communication problems in practice. In this context, the point in time matters when to integrate design activities, communication and comprehension problems as well as issues of linking organizational and structural aspects.

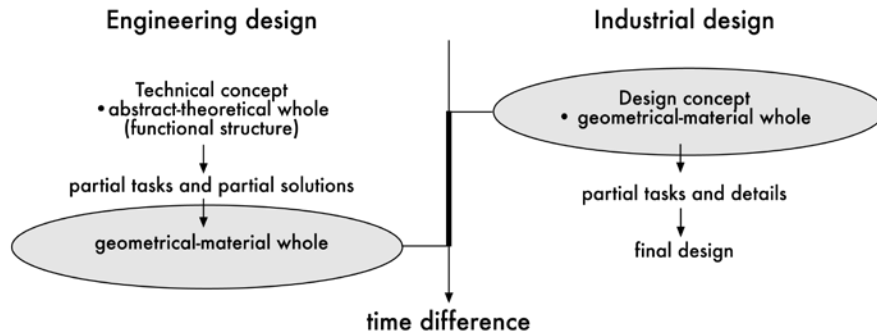


Figure 1. Different points in time at which the geometrical-material entity is created [1]

Figure 1 illustrates this fundamental problem. During the design process, the designer creates a gestalt (form or shape) or a geometrical-material entity in the early design phases because it is the only way to analyse, evaluate, and further develop the overall impact of the design concept. Normally, engineering design concepts for the overall appearance of the future product (structural design, housing) do not exist at this point in time. Agreeing on the shape or form of the product (aesthetic design) and the design of individual components (engineering design) may become a problem with a high conflict potential.

In general, conflicts may arise from the following circumstances:

- increasing division of labor during design processes since the time of the industrial revolution until today;
- development of engineering design methods that disregard people's expectations as users of technical products and thus do not reflect human-related product requirements sufficiently;
- development of design tools geared to a strict division of labor;
- engineering degree programs in line with the model of the division of labor which paid little attention to user requirements (human machine interface);
- different degree or training programs for engineers and industrial designers.

Traditional engineering programs still comprise a number of fields of study that do not focus on the bigger picture (i.e. creating an overall design). In the case of architectural engineering, it is the architect who takes on the role of gestalt designer. The architect envisions the shape or form of a building. In engineering programs, industrial design should play this part. The different approaches to engineering design and industrial design are perceived as normal when they are explained in engineering and industrial design programs in view of their specific tasks. Once the foundations have been laid as described in [1] and [2], it is possible to create an understanding and readiness to follow an integrated approach in all phases of the design process.

Practitioners are all too familiar with the problem. The ideation of a form (gestalt), often in the shape of a final model of the future product, has increasingly become an important strategic and methodological instrument of the development philosophy. Design engineers and industrial designers who are only familiar with the approaches linked to “their” own methods are prone to conflicts. Finding common ground will take more time and incur costs if they do not recognize or accept this difference in order to overcome it.

1.2. Harmonization and collaboration requirements

There are a number of ways to help ease the relationship between design engineers and industrial designers during the early stages of product development. They include:

- raising understanding and providing information about training and qualifications of each discipline,
- synchronizing development steps with many iterations,
- providing an integrated development environment (forms of organization, structural allocations, communication),
- providing a common data basis and efficient interfaces between digital tools (CAD, CAID, RP, model making).

Current product development philosophies accept the different points in time mentioned and describe a development environment encouraging collaboration between engineers and industrial designers.

The *Magdeburg Model of Integrated Product Development* [3] created the prerequisites for the integration of industrial design courses into an engineering degree program. It has been implemented successfully as part of the Integrated Design Engineering (IDE) master’s program.

2. TEACHING AND STUDYING IN AN INTEGRATED ENVIRONMENT

In 2000 the Faculty of Mechanical Engineering at Otto-von-Guericke-University in Magdeburg introduced the Integrated Product Development (IPD) area of specialization within the graduate program in General Mechanical Engineering. The way was paved by new design engineering research and university teachers who were open to an integrated approach to the product development process.

Until then the field of industrial design had played an isolated role. Now possibilities opened up to truly link the technical and the design-oriented development process as a study and research task.

2.1. Scientific foundations of Integrated Product Development (IPD)

Olsson was the first to publish the basics of IPD at the University of Lund (Sweden) in 1969. Since then, IPD has been further advanced in many ways. The Magdeburg approach to IPD was described in detail by BURCHARDT and

VAJNA [4]. It paved the way for an integrated approach to engineering studies at the University of Magdeburg.

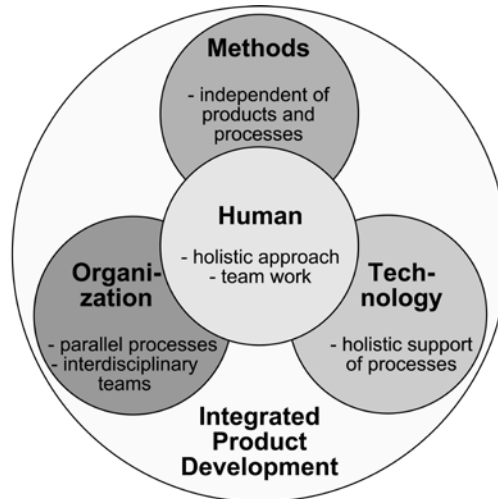


Figure 2. The Magdeburg model of Integrated Product Development (according to [3])

VAJNA describes the following characteristics:

Human focus: All considerations are based on the assumption that human beings are creative problem-solvers. They come up with holistic solutions, acquire the necessary knowledge, use it to solve problems, and pass it on after finishing the task. Depending on the problem to be solved, a person can either work alone or in a team. During work, people communicate with internal and external partners in line with a holistic communication approach.

Field integration: All fields involved in product development are integrated in the product development process. These fields include sales and marketing, *industrial design*, development and engineering design, work preparation, manufacturing, assembly, shipping, maintenance, customer service, and product return. This makes it possible to largely take into consideration the impact of subsequent phases of the product's life cycle at a very early stage and make decisions at the earliest possible moment.

Product integration: In terms of product development, a product's shape, function, handling, product efficiency, sustainability, and good price performance ratio all have the same importance and impact since they influence each other.

Process integration: Making sure that all necessary steps are taken together and simultaneously in order to ensure the complete development and manufacturing of

the product. Processes can be understood as complex networks. If needed and appropriate, elements of such processes can be synchronized to a large extent.

Integration of methods: A number of flexible and efficient problem-solving methods as well as creativity and learning techniques are available for IPD and can be used depending on the context.

Knowledge integration: Providing comprehensive knowledge about the product, related development, manufacturing and usage processes and related methods and technologies in a knowledge base with such knowledge being acquired and transferred by holistic means of internal and external communication.

Application integration: Use of computer-aided technologies for (almost) every step of the development process within a jointly used user interface to dynamically model, simulate, and optimize the product's shape, features, behavior and its manufacturing and usage processes.

Information integration: Uniform, complete, consistent, and permanent information base for redundant-free storage and the avoidance of overlaps to the extent possible.

Generalization: IPD can be used for creating any kind of object (physical products, services, software etc.).

2.2. Integrated Design Engineering – an interdisciplinary course of study

The Chair of Information Technologies in Mechanical Engineering at the Institute of Mechanical Engineering is the driving force and main supporter of the IDE program platform. Current design engineering research, collective, practical experience in design engineering, industrial design related project work, and the introduction of the IDE master program manifest the transition from IPD to IDE.

Currently, two qualified industrial designers take responsibility for the study and research field of industrial design. The integrated study program focuses on development projects carried out by students. It links all theoretical knowledge taught in lectures with concrete assignments that companies provide in order to have a product newly developed or further advanced. The search for and selection of project partners focus on small and medium-sized companies from Saxony-Anhalt. The IDE projects help companies with product ideation, creating aesthetic, technical and ergonomic designs and obtaining intellectual property rights. In order to reach marketability, initial IPD product developments receive government subsidies. But contractors also include market leaders looking for fresh ideas and alternative concepts to in-house developments. Whereas IPD was only available to mechanical engineering students in the past, it has gradually become a highly accepted cross-departmental and interdisciplinary study program [2].

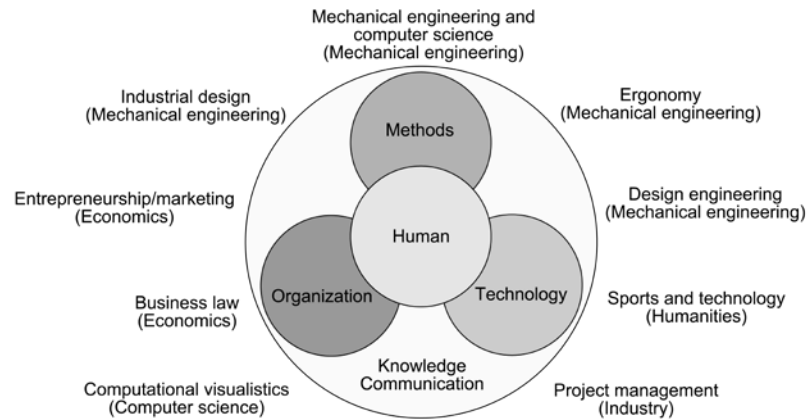


Figure 3. Where teachers and students of the IDE master program come from (according to [5])

In summary, the following characteristics make this study program special:

Heterogeneity: IDE teachers represent various disciplines and faculties. Coursework includes special design seminars where students can learn to apply a multitude of different design methods and tools.

Project work: Students from participating faculties work together in heterogeneous teams. Typically, assignments for developing a new product or modifying an existing one come from companies. Market analyses, intellectual property rights and usage analyses, drafting, designing a preferred option, and building a model or functioning prototype are important steps in the drafting and design process. The results must be defended in front of an expert jury after having reached different milestones.

Coaching: Each student project is coached both by research assistants from various fields and an industrial designer.

Internationalization: In some cases, projects are organized together with student teams from foreign universities. We had international project teams with students from the University of Miskolc and the Technical and Economic University of Budapest (both in Hungary), the FONTYS Hogeschool in Eindhoven (Netherlands), Lehigh University of Bethlehem, PA, USA, INGP Grenoble, ECP Paris (both in France), the University of Malta, and Carnegie Mellon University of Pittsburgh, PA, USA.

With the publication of the book *Integrated Design Engineering – ein interdisziplinäres Modell für die ganzheitliche Produktentwicklung* [1] there is now also a textbook available for Integrated Design Engineering.

3. DESIGN SPECIALTY WITHIN AN ENGINEERING PROGRAM

What is possible, what makes sense?

Time constraints in design coursework, the study intentions of the students and their individual prerequisites are conditions that may limit possibilities but also present opportunities for trying something new.

3.1. Objectives and focal points

From the many approaches implemented since 1984 within the degree program at the University of Magdeburg, a relatively fixed curriculum offering more than 10 different mandatory classes and electives has emerged and become a staple of the Magdeburg engineering program.

Put in a nutshell, objectives and focal points include:

- introductory knowledge about industrial design,
- creating awareness of design challenges in product and environmental design,
- exploring design philosophies, quality standards and positions on contemporary product and environmental design,
- presenting justifiable positions to counter an anything-goes-approach to industrial design,
- acquiring knowledge to be able to consider and to integrate design challenges in the context of engineering decisions,
- touch-point issues between industrial design, design engineering, manufacturing, ergonomics, marketing, and ecology,
- analysing and designing usage processes (in terms of the perception of action and object perception) as an especially important aspect of the design process and source of decisive gestalt requirements,
- the specificity of the design challenge: creating perceptually adequate designs,
- creating awareness of aesthetic design with an understanding of perceptual adequateness to complement technical design requirements such as adequate load, material and production requirements,
- design exercises: training the eye and the hand,
- concrete and applicable advice for designing products with design theory in mind,
- real experience in applying integrated approaches by participating in interdisciplinary and cross-departmental projects,
- practical training through participation in corporate product development projects.

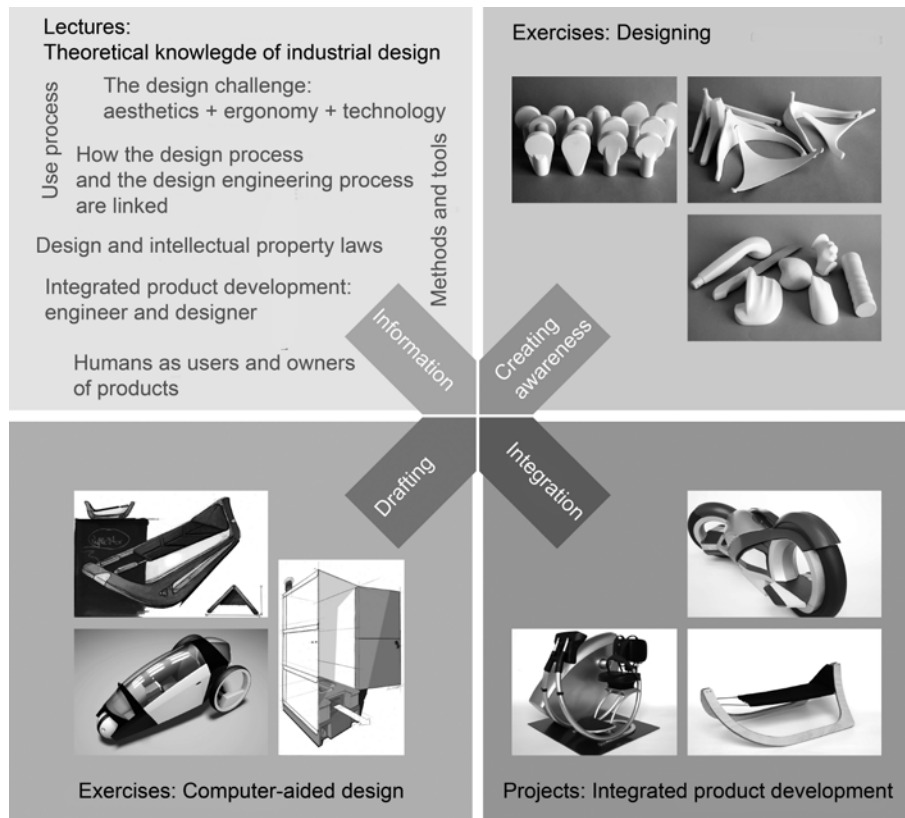


Figure 4. The four elements of design coursework [8]

A design specialty integrated into an engineering program requires a specific selection of topics geared to the requirements of the engineering program. Touching points between industrial design and design engineering are defined by their object and process-related nature.

The product design coursework aims at four aspects shown in *Figure 4*.

1. Providing knowledge about industrial design during lectures.
2. Creating awareness of design qualities in practical exercises.
3. Practicing drafting techniques such as sketching, drawing, computer-aided visualizing and model making.
4. Learning to develop products in an interdisciplinary team.

Over the years, three main topics have emerged forming the core of the current curriculum:

- considering the use scenario as a design challenge,
- creating perceptually adequate designs, and
- pursuing an integrated approach.

These three topics are barely touched or not taught at all in traditional engineering programs. Since they all focus on people as users of products, industrial design can make a valuable contribution to engineering programs.

3.2. The use scenario as a design challenge

Engineering studies approach technical objects such as machines and devices in view of their hardware performance, thus neglecting the human-machine interface. Increasing automation and electronification (miniaturizing and digitalizing) obscure questions of user-friendly design. However, it is possible to counter trends towards so-called black box design (standardization and anonymization) by thoroughly analysing all human-related product requirements. If both design engineers and industrial designers concentrate on this aspect, there is a chance of finding consistent gestalt concepts. Schürer aptly describes this phase as “from the digitalized function to analogue action“ [7].

The use scenario as a basis for analysis and design ties together aesthetic, ergonomic and perception-related psychological aspects. By analysing the use scenario during the design phase, it is also possible to overcome the separation between design and ergonomics.

“In this sense, ergonomics can be understood as a design component, and aesthetics, in turn, as a component of ergonomics. However, in this context the aesthetics of an object must not be understood as associative aesthetics or pretty design but as an aesthetic related to and guiding action. It has not only an impact on how we experience the object but also on how we behave in the light of these aspects and, last but not least, on how we take targeted action. Experiencing, behaving and taking action are basic human experiences. It does not suffice to satisfy these basic needs by designing adequate artefacts for use that means ergonomically adequate devices. Instead these needs are essentially influenced by the creation of action-guiding elements, so to say in terms of their software ergonomics, that appeal to the senses [7].”

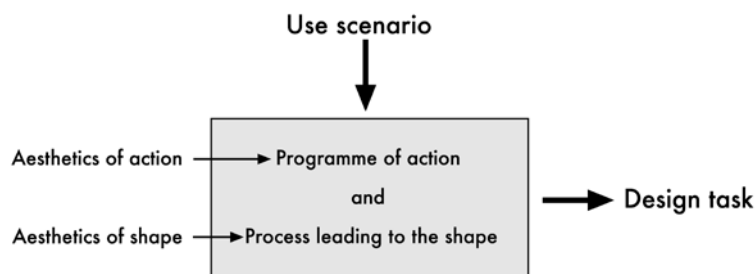


Figure 5. Use scenario as a design challenge [6]

The design task focuses on the user’s holistic perception and experience during use. The logic, sequence and understandability of usage and resulting behaviours as well as the search for the shape, colour, material, surface, and appearance of the

physical manifestation of the human-product interface must be taken into consideration.

A design assignment described as such would be too narrow for a university design program, but has proven to be useful for a design specialty within an engineering program in my experience.

If we want to develop actions and forms that are usable, we need to ask ourselves how we “use” a product. During the development process, all prerequisites and requirements are planned so that the user can later experience what it means to “see” and “operate” the object. Perceiving and sensing harmony, pleasant feelings and grace but also to experience contrasts and tension stimulates the senses leading to a unique user experience.

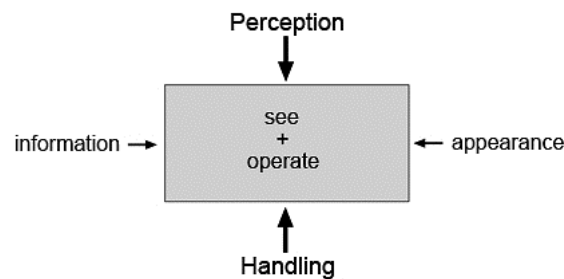


Figure 6. Relation between use-related action and design field [6]

To implement this approach, it is necessary to describe design objectives and quality standards based on questions such as:

- What is perceptually adequate?
- What satisfies appearance requirements?
- What satisfies information requirements?
- And what eases handling?

The didactic approach illustrated up to this point raises the students’ awareness of all questions related to the product’s future use.

It is not difficult to teach engineering students that understanding a technical product’s future use is important because engineers can typically emphasize with the role of the user if asked to. Industrial designers will continue to be experts for such questions. Projects have shown that designing a use scenario together is an interdisciplinary effort and can therefore have a highly integrative effect.

3.3. Functional AND usable form as an objective

Design engineers design technically defined forms. A substantial part of engineering coursework deals with design engineering and technical design requirements. Defining adequate loads and meeting material and production specifications are requirements that directly manifest themselves in the embodiment of components, assembly groups, and holistic product forms. A form developed in such a way may be referred to as a functional form.

A functional form is not a usable form yet, especially not if products with distinctive human-product interfaces are concerned. In case of many technical objects, form and content do no longer correspond. There is a tendency towards an arbitrariness of form. To counter this trend, we need to formulate well-reasoned positions for a clear design responsibility. The objective must not be black box designs but forms that stand the usability test and touch the user's senses.

To reach this goal and understanding within the study program, students are introduced to the theory of form. Based on this way of perceiving forms and their impact on human beings, they are challenged to analyse, draft, and reify design ideas.

At a theoretical level, students study how shapes develop and are created, they are introduced to form methodology (form features), form systematics, and quality criteria of perceptually adequate designs.

Based on this knowledge, it is possible to formulate and solve very practical design challenges in the context of creating perceptually adequate designs.

To what degree is it possible to explore the depths of aesthetic design within an engineering program? It is useful to be aware of these connections but it does not suffice to come up with a creative solution to complex design challenges. A professional design competence will develop only based on virtually available design knowledge, personal sensory-creative prerequisites, and a wide range of technical skills (design tools).

Engineering programs do not offer this combination. It is also not the goal of the curriculum. So what is possible and makes sense?

Typically, an engineer is familiar with her/his design requirements that ideally help her/him to come up with a functional form. S/he should understand that the human being is the measure of all things and s/he should have an idea of cause-form/effect aesthetics. Additionally, s/he should also know how a design engineer can influence a user-oriented design.

Following this approach, students are introduced to a multitude of criteria, information, and recommendations available in texts and images on perceptually adequate design. Central topics include:

- recommendations on gestalt creation with regard to an entire object or elements of an object,
- recommendations on gestalt structuring,
- recommendations on organizing forms.

Such an approach as described above follows the vision of understanding functional form, usable form, and formal-aesthetic form as a sensory entirety and links it with the requirements of a technically determined design during the design process.

Subsequent design exercises produce results on a sensory level that can be evaluated. What impact has an edge, a surface, or a transition of forms? How do I find out the correct gripping volume? Does it feel organized or too complex? How can I

organize a form? These are all questions that an object raises, which students can see and describe.

Making and working on an object is already a way of generating understanding. Students can experience what it means to “think with your hand”. They learn to understand their eyes and hands as sensory tools. These exercises do not suffice to teach design competences on a degree level but they are ideal for illustrating the sensory-aesthetic challenge by giving students a chance to learn by experience. In addition to creating sensory experiences, e.g. by touching a well-designed handle, students also learn to verbally describe their work since the right terminology is necessary to be able to describe and evaluate designs.

3.3.1. Design exercises

On a didactic level, exercises focus on making, perceiving and evaluating objects. Methodologically, they are based on the theory of form. *Figure 9* illustrates the design categories applied to a model.

The methodology follows the principle of simplicity to complexity.

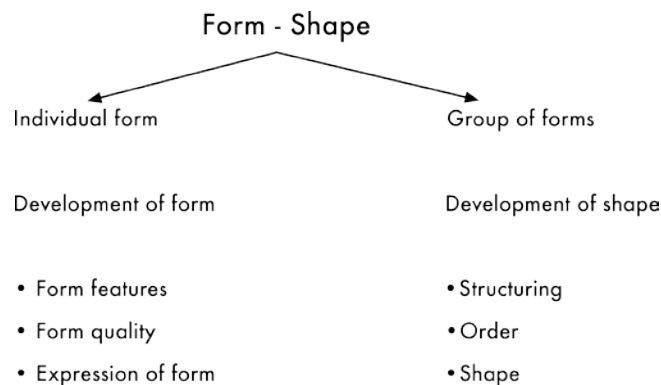


Figure 7. Methodological approach: design exercises [6]

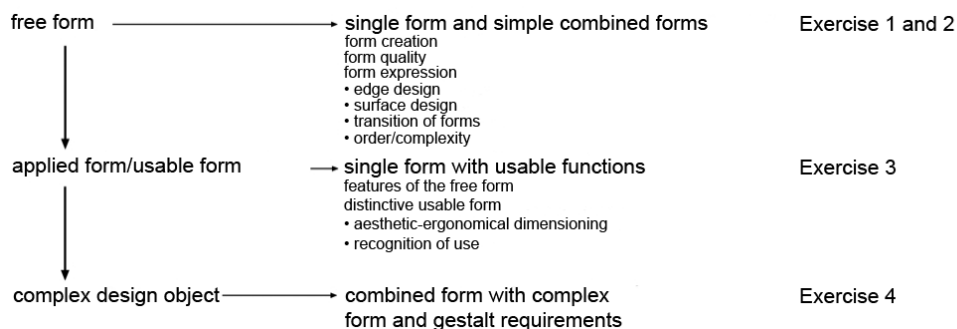


Figure 8. Topics related to the theory of form [1]

The following images illustrate the results. The complexity of the design assignment increases from left to right.

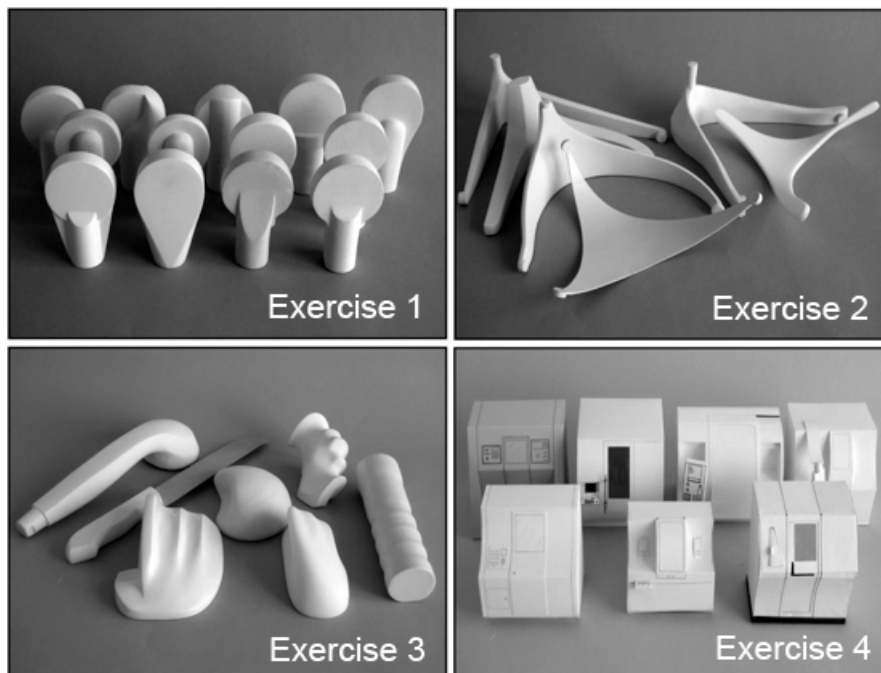


Figure 9. Design exercises – Models made of plaster and paper [6]

3.4. Sustainable design

In recent years, interest in sustainable product development has increased tremendously. Development objectives related to the use, manufacture, trading, repair, and disposal of a product must be integrated into the early phases of product development. This raises questions directly related to product design.

Sustainability aspects such as:

- Compostable: Products whose organic elements are transformed into soil by living microorganisms at the end of their use.
- Long product life: Long-lasting products as an expression of the sensible use of natural resources (can be repaired, cleaned, recycled, not a fad).
- Local: Use of local material, strengthening local businesses.
- Saving energy: Low energy consumption, scaling down the carbon footprint.
- Avoiding trash: Reducing scrap, increasing recycling, useful packaging.
- Multiple use: Used several times, combined use.
- Recyclable: Products that can be used to generate new raw material once they have reached the end of their product life.

- Up-cycling: Making new products from old products.
- Renewable resources: Products made of material that replenishes naturally.

Coursework is divided into lectures and small projects on the sustainability aspects listed above.

4. IDE DEVELOPMENT PROJECTS FOR STUDENTS – LEARNING HOW ENGINEERS AND DESIGNERS CAN CO-OPERATE

In many cases, project teams are composed of students studying the disciplines shown in *Figure 3*. The core of a team is made up of students majoring in IDE, mechanical engineering, computational visualistics, sports and technology, and industrial design. Other team members may study occupational psychology, marketing and entrepreneurship.

The fact that industrial design majors studying at the Institute of Industrial Design of the University of Applied Sciences of Magdeburg/Stendal also participate in these projects is a hallmark of the model. To have future engineers and designers meet during their studies is a great way to teach students how to smoothen the product development process. Bringing together different approaches to designing, special knowledge and methodological skills and tools are both an opportunity and a risk of such co-operation.

4.1. Experiences of an integrated approach for engineering and/or design majors as illustrated by the example of the main phases of the design engineering process of an IDE project

In the weekly team meetings, students discuss the technical input by all students participating in the design process, their specific perspectives on the challenge at hand with the aim of finding a solution that they can all agree on.

Analysis phase: A division of labor largely characterizes work in the analysis phase. Design majors research forms and uses of previous products or competing products. Future engineers analyse performance parameters, technical principles, the design of individual components, and materials to be used. Together they carry out intellectual property rights analyses. Based on further analyses (market analysis, customer surveys, company research etc.) they define the assignment and present a design brief at the first milestone meeting. Typically, no conflicts arise during this phase.

Conceptual phase: During the conceptual phase, ALL students must present their ideas and first sketches during the meetings. As shown in *Figure 1*, conflicts regularly surface. Engineering majors focus on technical details. Their excessive self-censorship with regard to costs and implementation limits their creativity. Often they are not able to make convincing sketches. They turn to computer-aided designs and calculations for reassurance but these often come too early in the process. Industrial design majors typically present skilful sketches and visionary holistic de-

signs. This is the point when students, guided by an experienced facilitator, need to learn that their own (learned) approach must be harmonized with the approaches pursued by the other team members. For industrial design majors it is oftentimes hard to understand and personally painful to have their first sketches attacked by arguments they perceive as absurd and pointless. This is when it becomes obvious that they have not been prepared for such a confrontation.

Engineering majors must learn that in the early phases of product development, the search for holistic technical and aesthetic concepts takes centre stage and that questions of the product's usage characteristics for the user are more important at this point than, for instance, optimizing a component. By developing a use scenario together, students have a chance to fuse aesthetical, ergonomic, occupational, psychological, and technical requirements. The path to a usage and a gestalt vision is strewn with conflict but it is the right path leading to a feasible and acceptable integrated design process. The use scenario developed together opens the view to the problem at hand. It makes it easier to organize, structure, and evaluate the ideas and concepts the students have come up with. The step of developing one or several preferred concepts remains a challenge, however. But the use and gestalt vision presents an objective that guides the selection process. The conflict potential decreases significantly; the development process becomes more target-oriented and efficient.

In summary, it should be noted that the concept phase brings familiar conflict patterns to the surface. By developing the future usage scenario together, engineers and designers can come up with a mutually agreed design vision. All subsequent processes will be less prone to conflict and more efficient. This phase takes three to four weeks and ends with defending the 2nd milestone.

Design phase: Once this phase has been reached, students (should) have achieved a good balance between an integrated and a subject-specific design engineering approach. The engineers continue advancing the technical concept, dimensioning components and making calculations based on the designers' form and detailed sketches. In order to meet ergonomic requirements, the engineering design and the aesthetic design need to be adjusted and modified constantly. Production-related and economic conditions are gaining more weight and must also be taken into consideration in the engineering and aesthetic design. What is typical of this phase is the digital exchange of design data between engineers and designers (and computational visualistics/IT specialists). The students are trained to use special computer technology. The exchange of design data has become increasingly easier thanks to advanced data transfer technology but it still takes up time and resources. After about 7 to 9 weeks of integrated project work, students collaborate increasingly with regard to the drafting, selection and evaluation process. They deal with conflicts more productively, i.e., individual skills and competencies flow directly into the creative teamwork. Once the 3rd milestone is reached, a design concept agreed by all students is presented illustrating all technical and design aspects (CAID and CAD images, physical models, calculations, evaluations, selection processes).

Documentation phase: Again, a division of labor characterizes this phase. Engineering majors are responsible for making CAD drawings and a functional model. Functional models are used to prove the selected technical concept in terms of its functionality and usability. Typically, these workshop models combine the main functional components and make initial functional tests possible but they still lack an aesthetic design quality. Industrial design and computational visualistics majors prepare high-quality renderings, animations, and presentations. Often students studying design engineering and/or industrial design work together on the model. Increasingly, rapid prototyping models serve as a basis for final models.

A complete product documentation normally comprises:

- project management documentation,
- presentation and evaluation of all analyses,
- documentation of the technical and industrial design across all phases,
- functional and design models,
- final report provided by the team leader.

Presentations open to the public at the university or in R&E departments mark the highlight of the semester project work. In many projects, student teams also come up with a marketing and business concept for the same product development assignment. Since these concepts also span all milestones, students gain an excellent understanding of all phases of the product development process.

5. SUMMARY

At the beginning of the 1990s, the University of Magdeburg started to offer industrial design courses for mechanical engineering majors in addition to traditional engineering programs. Finally, in 2000 after several failed attempts of integration, IPD was introduced as a specialty within the mechanical engineering program.

After the introduction of bachelor and master's programs around 2009, the study course and research platform *Integrated Design Engineering* developed providing an ideal platform for integrating industrial design coursework into the engineering program. Graduates of the Integrated Design Engineering master's program have gained and are able to apply the skills needed to work on and advance the touch points of engineering design, industrial design, and ergonomics especially in the early phases of product development.

REFERENCES

- [1] GATZKY, Thomas: Produktdesign (Section 3.2.1) und Industriedesign (Chapter 4). In: VAJNA, Sándor (Hrsg.): *Integrated Design Engineering. Interdisziplinäres Modell für die ganzheitliche Produktentwicklung*. Springer, Berlin–Heidelberg, 2014.

- [2] NAUMANN, T.–GATZKY, T.–VAJNA, S.: Integrierte Produktentwicklung als Ausbildungskonzept. *CAD-CAM Report*, Jg. 23, Nr. 2, 2004.
- [3] BURCHARDT, C.: *Ein erweitertes Konzept für die Integrierte Produktentwicklung*. Dissertation. Otto-von-Guericke-Universität, Magdeburg, 2000.
- [4] VAJNA, S.–BURCHARDT, C.: Ein erweitertes Konzept für die Integrierte Produktentwicklung. In: VAJNA (Hrsg.): *Buchreihe Integrierte Produktentwicklung*. Band 3. Otto-von-Guericke-Universität Magdeburg, Reihe Magdeburg, 2001.
- [5] VAJNA, S.–NAUMANN, T.: Implementation of the New IPD Study Course at the Otto-von-Guericke University Magdeburg. In: CULLEY, S.–DUFFY, A.–MCMAHON, C.–WALLACE, K: *Design Applications in Industry and Education. Proceedings of the 13th International Conference on Engineering Design 2001 (ICED 01)*, 277–284.
- [6] GATZKY, T.: *Vorlesungs- und Übungsmaterialien zu den Lehrveranstaltungen Industriedesign*. Technisches Design für Ingenieurstudenten der Fakultät Maschinenbau an der Otto-von-Guericke-Universität Magdeburg, 2008.
- [7] SCHÜRER A.: Entwicklungstendenzen im Investitionsgüter-Design. Designcenter Stuttgart (Hrsg.): *Design aktuell*, 1, 1988.
- [8] GATZKY, T.–WIESNER, M.: *Dokumentation und Ausstellung zu „30 Jahre Industriedesign an der Otto-von-Guericke-Universität Magdeburg“*. 2014.

Translation by Dr. Janina Gatzky

EXAMINATION OF SUITABLE METHODS FOR DESCRIBING MACHINE TOOL STRUCTURES

RÓBERT KISS–GYÖRGY TAKÁCS

*University of Miskolc, Department of Machine Tools
3515 Miskolc-Egyetemváros
kiss.robert94@indamail.hu, takacs.gyorgy@uni-miskolc.hu*

Abstract: The objective of this paper is to describe suitable methods for the serial and parallel kinematics machining centres. These have an important role in the examination of the machine, since the structure equation of different varieties of machine tools may already be established during the period of design. An additional argument is that the main components can be purchased from the manufacturers specialized on manufacturing such units of that the structures can be built up by certain principles, such as the modular principle. For this reason, the most important part of the design process is now to reveal new structure varieties with the application of structure delineation methods. Nowadays, the machine tool constructors are mainly engaged in this area.

Keywords: *machine tool, methodical design, SKM, PKM, HKM*

1. INTRODUCTION

Basically one can distinguish two different machine structures. These are serial and parallel machine structures, but there are hybrid ones too (Hybrid Kinematics Machine tools), which are made up from the combination of the foregoing. For describing this kind of machines a variety of exploratory and descriptive methods have been developed. The primary goal is to describe these methods in the paper, furthermore these examinations and assessments according to [1], [3], [4] and [5].

2. SERIAL STRUCTURE MACHINES – SKM¹

Analysing machining centres with serial built structure, machine-specific kinematics are similar to building a chain i.e., the elements that make up the modules are connected to each other directly, so it will be a serial arrangement of the structure (*Figure 1*). The kinematic chain consists of two parts. One end of the chain there is the tool, on the other side is the workpiece. As the individual components are building on each other, we receive a lot of different structures of machine tools.

¹ SKM – Serial Kinematics Machine tools

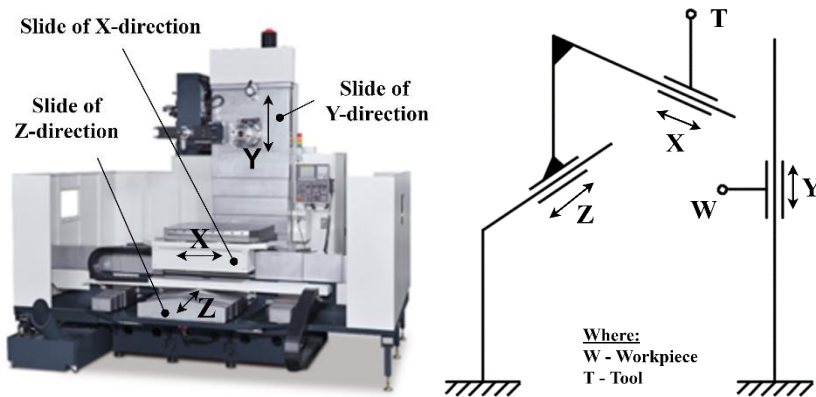


Figure 1. Machining centre: a serial structure with its kinematic model

3. PARALLEL STRUCTURE MACHINE TOOLS – PKM²

The construction of the parallel kinematics machining centres is relatively novel in the field of machine tools, which, due to some certain benefits to SKM, are significant. For example, the high cutting speed, feed and rapid traverse rates, the dynamic stiffness for precise trajectory tracking.

For the machine frame structure joints fixed by the actuators are connected to a common platform, and their simultaneous and coordinated motions set up the relative displacement of the tool and the workpiece.

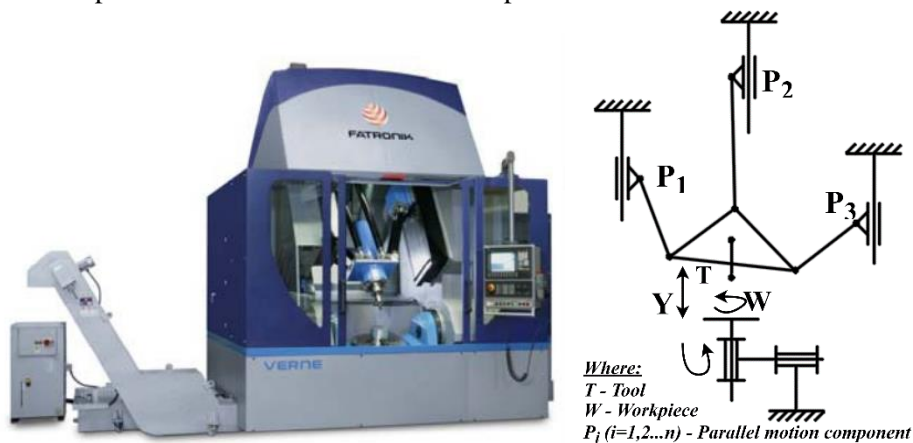


Figure 2. 5-axis PKM and its kinematic model [2]

The main disadvantages of this structure is that the size of the effective work space is small compared to the machine size, singularities and blind spots occur in the work area, complex machinery calibration, furthermore the machine functioning is

² PKM – Parallel Kinematics Machine tools

very complicated (5-6D even for linear interpolation), which requires expensive control device.

Machining centre seen in *Figure 2* unfits for the application of serial specification description method, these structures can be described with description matrix and graphs very well. The description of the method is discussed later. *Graph helped writing off method* is a perfect mean for this type of machine tool structures.

4. HYBRID STRUCTURE MACHINE TOOLS – HKM³

In order to take advantage of the useful properties of both structures, the hybrid structure machines are made up of a combination of serial and parallel structures.

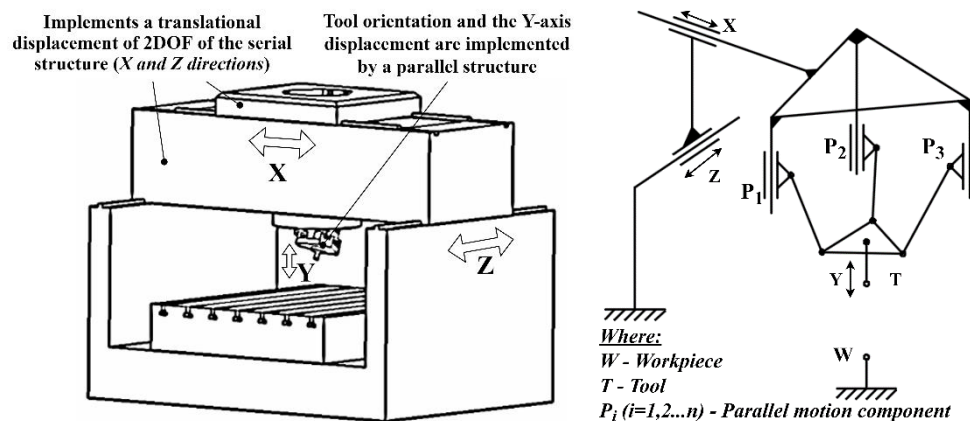


Figure 3. Sketch of hybrid structure and kinematic model of these machine tools [6]

These hybrid structures are widespread used in robotics, for example the machine in *Figure 3* which displays a multi-axis machining system. In this case, serial structure implements the two degrees of translational motion (*X and Z*) and then followed by a parallel structure, which is next to the *Y* in the translational motion of the tool orientation.

5. METHODS USED FOR DESCRIBING MACHINE TOOL STRUCTURES

This chapter contains the known descriptions of structures which are the *description on the level of sharing displacements and priority* [4]; the *neighbour method* [1], [3] and the *graph helped writing off method* [5]. All three versions are suitable for exploring and describing machine structure serial versions, but to analyse the parallel or branching structures, the graph helped writing off method may only be suitable.

³ HKM – Hybrid Kinematics Machine tools

In the course of researching foreign literatures, YOSHIMI developed the method that was very similar to the graph helped writing off method, making it also suitable for branching and parallel kinematic machine centres. In this article this method will not be discussed, since now we analyse only Hungarian researches.

Moreover, a machining centre, therefore a particular serial structure (*Figure 1*) will be presented in the structure equation, the previously mentioned three methods. Some comparative basis the structure equations are also displayed for which the code structure, complexity and variety of machine tool characteristics taken into account.

In *Figure 1* a CNC machining centre is shown, where the cutting movements are done by two directions of the workpiece and one directions of the tool. The work table moves in the horizontal plane.

5.1. Description of level of share movements and priority

TAJNAFŐI [4] at the University of Miskolc Department of Machine Tools defined the principle of the serial kinematic machine tools. Any of these structures is a chain of members built on each other, and which members provide an elementary displacement, and where one of the elements is fixed to the ground, and one of the end of the chain holds the tool, while the other carries the work piece. It is a useful method for structural analysis, which makes it possible to analyse machine structures theoretically by the means of exploration and combinatorial analysis. It is a universal method, which is suitable for describing the structure of any serial device.

Cascading machine elements built on each other are indexed by letters and the Z axis of the coordinate system is always parallel to the main spindle.

Therefore, by applying the method seen in *Figure 1* machining centre, we obtain the following result:

- The tool performs the movements, so the Y direction's priority is: 1 (*maximum value*), as part of the chain length of the tool kinematics: $1 \rightarrow Y_{s1}$.
- The workpiece performs displacements long the X-axis first, and then along the Z-axis, thus the priority: X is the first, Z is the second part of the chain, and the length of the kinematic chain: $2 \rightarrow X_{m1} Z_{m2}$.

As a result of the logic mentioned above is the structural equation of the structure seen in *Figure 1*, which can be set up as follows:

$$X_{m1} Y_{s1} Z_{m2} \quad (1)$$

$$X(m,1) Y(s,1) Z(m,2) \quad (2)$$

5.2. Neighbour method

This method has been developed by LIPÓTH [1]. Quality is capable of being taken into account by using 10 parameters for the descriptive equation in the course of exploring variations. The title of the subchapter also refers to this, since this method applies the relationships between the building blocks. With this method, kinematics can be built up of open chain consists of only four members. Where the four members are: M (*main spindle*), MN (*main spindle neighbour*), TN (*table neighbour*), T (*table*). You can see the elements on the basis of these neighbouring relationships. In addition, the three linear directions of motions of the guides may be set according to the following: TL (*top line*), ML (*middle line*), BL (*bottom line*).

During the application of the test method, the analysed basic machining centres do not carry any tool magazine or pallet-table, and the tool performs only 3 linear motions in relation to the workpiece, so do not deals with real machines used rotary tables and tilting heads.

Guides are used for linear movements by connecting two-two members together. So machining centres are built up of a four-member open chain connected by three guides. At one end of the chain there is the slide with spindle which carries the tool, at the other end the workpiece carrier table.

Due to some reasons coming from measurement-technique, the 3 motions are perpendicular to each other and one of them is directed vertically. Each important direction of a machining centre can be connected to the Cartesian coordinate system joined to movement directions. The spindle axis is always parallel, while the normal vector of the table is perpendicular to any of the directions.

Table 1
Symbol system of the method

Parameters	Possible value				Details
<i>not_move</i>	M	MN	TN	T	The fixed member of the kinematic chain.
<i>spindle_axis</i>	TL	ML	BL		The spindle axis which is parallel to the guides.
<i>up_down</i>	TL	ML	BL		Determination of the direction of the vertical direction.
<i>table_normal</i>	TL	ML	BL		The work surface which is parallel to a normal guide.
<i>fv-normal</i>	ML		BL		The normal vectors of the planes of the guides.
<i>kv-normal</i>	TL		BL		
<i>av-normal</i>	TL		ML		
<i>fv-short</i>	M		MN		The element at which the short guide is placed in case of each individual guides.
<i>kv-short</i>	TN		MN		
<i>av-short</i>	TN		T		

The structure equation of the above mentioned machine (*Figure 1*) and which is based on *Table 1* is the following:

$$MN \ ML \ TL \ TL \ ML \ TL \ TL \ M \ TN \ T \quad (3)$$

5.3. Graph helped writing off method

This method is developed by TAKÁCS [5]. The novelty of the method is that, besides serial structures, it also can be used for both writing off parallel or branching structures. While using this method, members in the structure that are independent of their function should be suitable for determining special location of units. To this end, it was necessary to extend the code and more specifically to enable the computer automation, giving the connection of the elements independent from the role of an element within a structure.

Coding system details:

$$O_{m,s,i,\vec{k}} \quad (4)$$

Where:

O – the expression that defines the function of the system

i – priority

w, t – workpiece or tool kinematic chain of the object

\vec{k} – list vector describing object relationships

If the machine, that we should like to implement, consists of predefined structure elements, we have to fix the elements of the set that we should like to take into account. In addition, we have to define how the elements are related to each of the other elements of the set.

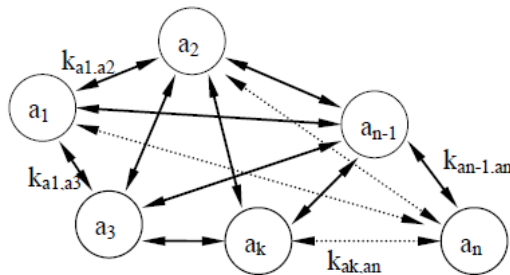


Figure 4. Machine structure described by graph

So we can get a complete graph, which is shown in *Figure 4* and the corresponding symbols are:

a_i ($i = 1, 2, \dots, n$) – the graph points, the building blocks of your machine tools

$k_{ak, an}$ – two-point edge in the graph select that contact between the two building block types

Each machine is part of the complete graph with advanced graph versions are created.

Elements connection description matrix can be described by the following way:

The matrix is characterized by the elements set to 0 or 1, depending on whether there is an element or not. Main diagonal contains no elements, it would not be meaningful, because they carry with them certain components to their own writing. The matrix is symmetric, since the connection between the elements is mutual and bidirectional. *K* graph may have a lot of adjacencia graph as the permutation of the rows and columns of *K* always determines a different matrix, but in its content does not change anything.

$$K = \begin{bmatrix} 0 & k_{a_1,a_2} & \cdot & \cdot & k_{a_1,a_n} \\ k_{a_2,a_1} & 0 & \cdot & \cdot & \cdot \\ \cdot & \cdot & 0 & \cdot & \cdot \\ \cdot & \cdot & \cdot & 0 & \cdot \\ k_{a_n,a_1} & \cdot & \cdot & \cdot & 0 \end{bmatrix}$$

Figure 5. Description matrix

Describing machine introduced in Figure 1 description using this method:

- Define the TA connectivity support: [0 1 0 0 1] = 34 ⇒ TA (w, 0, 34)
- Define the TO connectivity spindle support: [0 0 1 0 0] = 4 ⇒ TO (t, 0, 4)
- Define the X connectivity slide: [0 0 0 1 0] = 16 ⇒ X (w, 1, 16)
- Define the Y connectivity slide: [0 0 0 0 1] = 32 ⇒ Y (t, 1, 32)
- Define the Z connectivity slide: [0 0 0 0 1] = 16 ⇒ Z (w, 2, 16)

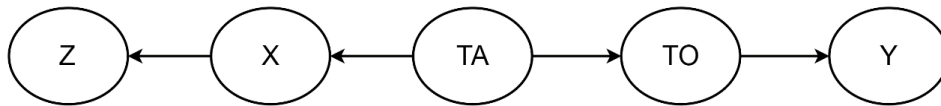


Figure 6. The descriptive graph of machine tool according to Figure 1

The following table describes the description matrix which illustrates the building blocks and the relationships between modules.

Table 2
Description matrix

	TA	TO	X	Y	Z
TA	–	1	1	0	0
TO	1	–	0	1	0
X	1	0	–	0	1
Y	0	1	0	–	0
Z	0	0	1	0	–

Using the above, the equation that describes the structure of machine tool introduced in *Figure 1*, is the following:

$$TA(w, 0, 34) X(w, 1, 16) Z(w, 2, 16) TO(t, 0, 4) Y(t, 1, 32) \quad (5)$$

6. THE ASSESSMENT OF THE DESCRIPTIVE METHODS

Table 3
Summary of the features of the methods

<i>Description on the level of shared movements and priority</i>	<i>Neighbour method</i>	<i>Graph helped writing off method</i>
2 parameters – assigned to coordinate axis – are taken into account (<i>index</i>).	Takes into account 10 parameters, which are equally ranked and there is no fixed parameter.	A code-system used by Tajnafői, extended by a \vec{k} vector, that describes the connections of the object.
Does not take into account the qualitative aspects (<i>level of share movements and priority</i>).	Is able to take into account the quality criteria (e.g. work restrictions).	Makes a selection of good solutions with the help of a programed set of rules. Uses description matrix and graph for writing off structures.
All number of the versions: 48 (<i>machining centres</i>).	All number of the versions: 6912 (<i>machining centres</i>).	All number of the versions: 342 (<i>in the case of the examination of the grinder family</i>).
Not automated by computer.	Computer aided (<i>AutoCAD+AutoLISP</i>).	Computer aided test (<i>AutoCAD + Visual Basic</i>).
Serial kinematic chain.	Serial kinematic chain.	Serial and branching (<i>parallel</i>) kinematic chain.

The *description on the level of share movements and priority*, you can see that there are two parameters, the method examines machining centres at the level of the share movements and priority. Only serial kinematic chain structures are used to describe: 3-axis machining centres, horizontal and vertical spindle arrangement considering 48 versions.

With the *neighbour method* several aspects can be taken into account, a much more complicated equation that describes by ten parameters, and thus be able to take into account the qualitative aspects of variations to explore. Parameters are equal; versions are not assigned to coordinate directions. Examining 3-axis machining centres, 6912 versions may be considered.

The *graph helped writing off method* parallel or branching structure of the machine can also be used, in addition to the serial structure of machine tools. It has been applied in the practice during the development of a grinding-family, which may be the case of 342 versions, but this is not comparable to the former methods.

7. SUMMARY

This article describes the different types of machine tool structures and their describing methods. In the case of a 3-axis machining centre, it describes methods of distillation of the various features, marking system and with the analysed methods the structure equation of the machine tool introduced in *Figure 1* has been defined. The differences between these methods are collected in *Table 3*.

Analysis of the structure of writing off methods revealed that in the case of today's modern machine tools the writing off with graph method is the most appropriate, because this method is able to handle the serial, parallel and hybrid machine tool structures.

8. ACKNOWLEDGEMENT

This research was supported by the European Union and the State of Hungary, co-financed by the European Social Fund in the framework of TÁMOP-4.2.1. B-10/2/KONV-2010-0001 'National Excellence Program'.

REFERENCES

- [1] LIPÓTH, A.: *Megmunkáló központ konstrukciós változatok módszeres előállítás és értékelése*. Kandidátusi értekezés. Budapest, 1993.
- [2] L. N. LIPÓZ DE LACALLE–A. LAMIKIZ: *Machine Tools for High Performance Machining*. Springer, 2009.
- [3] NÉMETH, I.: *Conceptual design of 3-axis machine tools*.
- [4] TAJNAFÓI, J.: *Mechanizmusok származtatás elméletének alapjai és hatása a kreatív gondolkozásra*. Akadémiai Doktori értekezés. Miskolc, 1991.
- [5] TAKÁCS, Gy.: *Szerszámgépek strukturális tervezése grafikus adatbázisokkal*. Egyetemi doktori értekezés. Miskolc, 1996.
- [6] Tsann-Huei CHANG–Kuan-Wen CHEN–Chao-An KANG: Gantry type hybrid parallel five-axis machine tool. *US Patent*, US6719506 B2 (2004. 04. 13.)

CONTACT MODELS FOR MIXED FRICTION SIMULATION

JAKOB MODER–FLORIAN GRÜN

*Chair of Mechanical Engineering
Montanuniversität Leoben*

Abstract: Due to legislative requirements companies are enforced to take on demanding engineering challenges in order to fulfil targets regarding CO₂-emissions and pollutions. Especially the automotive industry has come up with a range of technologies throughout the past decade to reduce the amount of exhaust gases.

Tribology has played an important role and will be significant in the future when it comes to creating environment-friendly machines. Especially machine elements, such as gears, camshaft or roller-bearings, which are referred to as non-conformal machine elements from here on, are heavily loaded and have to operate under severe conditions. Often this results in the energetically unfavourable mixed friction state, which means that the total external load is shared by the oil and micro contacts. The current work is focused on methods for modelling these micro contacts in order to take them into account in state of the art EHD (elastohydrodynamic) models. This enables an in depth analysis of highly loaded machine elements in order to optimize machine elements sustainably.

Keywords: *Highly loaded contacts, EHD, mixed friction, tribology, contact mechanics*

1. INTRODUCTION

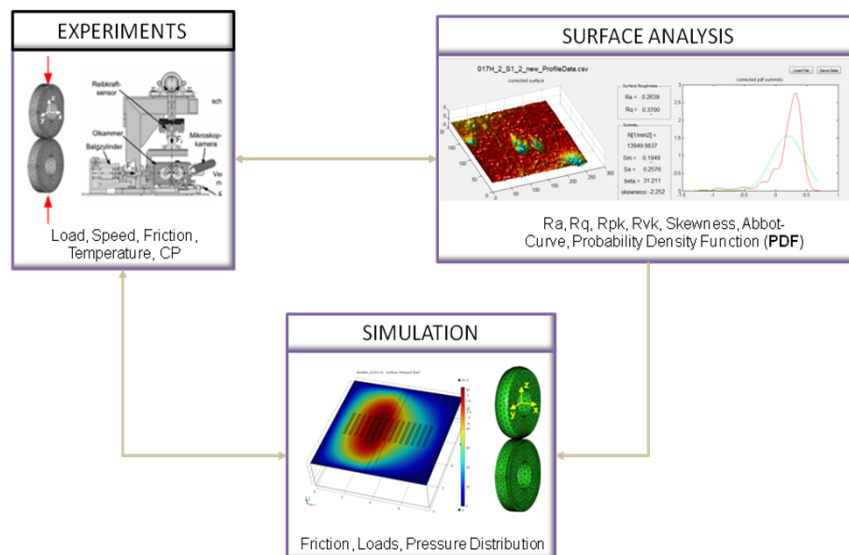


Figure 1. Applied Methodology

A comprehensive methodology, consisting of 3 major parts, has been developed throughout the last years at the Chair of Mechanical Engineering. *Figure 1* illustrates the methodology.

The methodology has been created to analyse the potential of different surface modification technologies (e.g. DLC coatings, micro structuring, superfinishing) in order to improve the tribological behaviour of non-conformal contacts. Discs are used as specimens, due to the straightforward manageability in terms of testing, machining and application of surface modifications. Nevertheless results can be transferred to actual machine elements.

In order to estimate which kind of surface processing technologies could be beneficial, simulations are carried out. They deliver information regarding pressure distribution, loads and friction. After a surface technology has been selected, the treated specimens are investigated by means of a laser-confocal microscope, which provides a 3D representation and various data off the disc surfaces. Finally, experiments are carried out in order to validate the simulation results and judge the suitability of the surface process for actual machine elements.

A key role in the simulation part is the accurate modelling of contact mechanics. However, since oil is always present in highly loaded contacts, complex interactions take place in this kind of tribological systems.

2. MIXED FRICTION MODELLING APPROACH

The idea of mixed friction modelling in general is, that the external load F_N is carried partly by the oil and asperity contacts of the mating surfaces. *Figure 2* illustrates this issue, by magnifying the contact area of a disc contact.

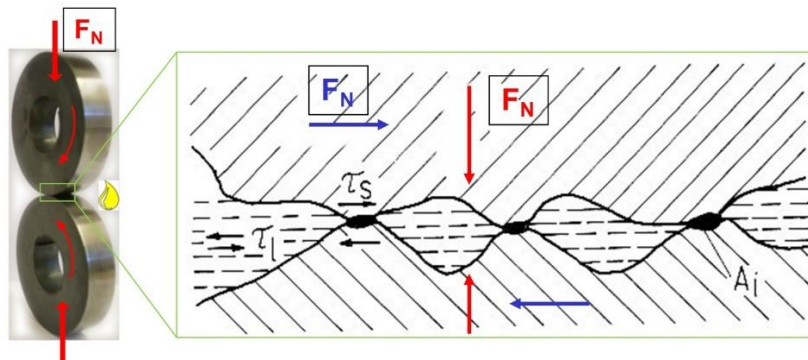


Figure 2. Mixed friction model approach [1]

Due to the relative motion of the surfaces friction is present. The friction can be split into two parts: τ_s which is resulting from the asperity contacts and τ_l which occurs due to the presence of the fluid in the contact. Complex interactions can

occur is this system, since the fluid directly affects the conditions for asperity contacts and vice-versa.

As a first step solely the contact mechanics problem will be dealt with, without taking into account the fluid and its properties.

3. STATISTICAL CONTACT MODELS

Statistical contact models make use of methods which describe technical surfaces in a statistical way, which means that contact problems can be dealt with in a relatively straightforward manner. In many cases analytical formulas can be applied in order to compute desired parameters.

The most popular model of this nature has been developed by GREENWOOD and WILLIAMSON [2]. It assumes that one surface is rough and that the other is perfectly smooth and rigid. The rough surface is transformed into spheres of a uniform diameter which behaves in a hertzian way. *Figure 3* illustrates how an actual rough surface is transformed into the model.

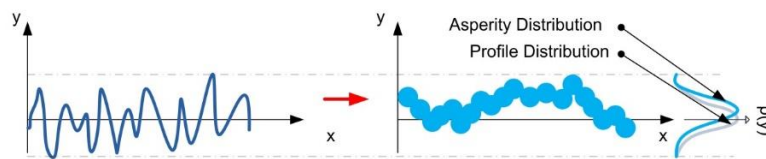


Figure 3. Model transformation

Figure 4 shows a description of the model. It also contains various elements which are important for analytical formulas which will be presented later.

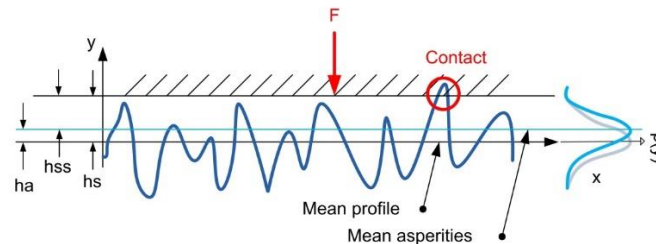


Figure 4. Model description

These elements are:

- mean value of profile,
- mean value of asperity (h_a),
- gap between mean of asperities and smooth surface (h_{ss}),
- external load (F),
- distribution of asperities $[p(y)] \Phi_s(y)$

Another important value is the mean sphere radius of the rough surface, which is denoted as β , and the number of asperities in contact which is called n .

Let y be the vertical coordinate of the surface and w the displacement in this direction, then for a specific distance h_{ss} w is:

$$w = y - h_{ss}$$

This results in a force acting on this asperity, which can be calculated as follows:

$$f = \frac{2}{3} E_r \beta^{1/2} w^{3/2} = \frac{2}{3} E_r \beta^{1/2} (y - h_{ss})^{3/2}$$

Taking into account that a technical surface has n asperities, the mean asperity pressure for the total contact can be computed as:

$$P = \frac{2}{3} n \beta^{1/2} E_r \int_{h_{ss}}^{\infty} (y - h_{ss})^{3/2} \Phi_s(y) dy$$

This method is very powerful considering that it is easy to handle and can still deliver accurate results, especially in situations where the load is moderate. However, non-linear material behaviour is not considered. The biggest drawback, however is, that each asperity is treated in an isolated way. Also it is not possible to evaluate local stresses in the contact.

4. NUMERICAL CONTACT MODELS

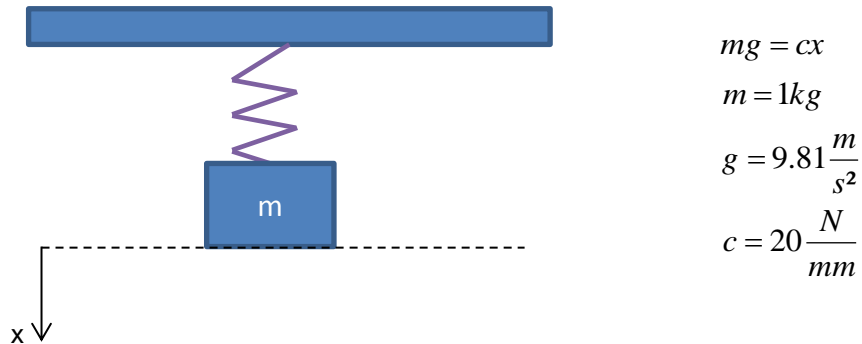


Figure 5. Spring mass system

Numerical contact mechanics has seen huge advances throughout the last couple of years due to the availability of huge amounts of computing power.

Nearly all methods are building on the Finite Element Method (FEM) which is based on the principle of minimum energy. The contact constraints are enforced by the formulation of an optimization problem.

In order to illustrate the problem, a spring mass system, as depicted in *Figure 5*, is considered. Due to the gravity and the spring, the mass will stay in a position x^* for the steady state case.

According to Newton the displacement of the mass is $x^* = 0.4905\text{mm}$

Another way to solve this problem is the usage of energy equations.

The spring energy is defined as:

$$S(x) = \frac{1}{2} cx^2$$

And the gravitational energy:

$$G(x) = -mgx$$

Therefore the total energy of the system is:

$$T(x) = G(x) + S(x)$$

Following the principle of minimum energy the stationary solution is:

$$\delta T(x) = 0$$

Figure 6 displays the total, spring and gravitational energy depending on the coordinate x .

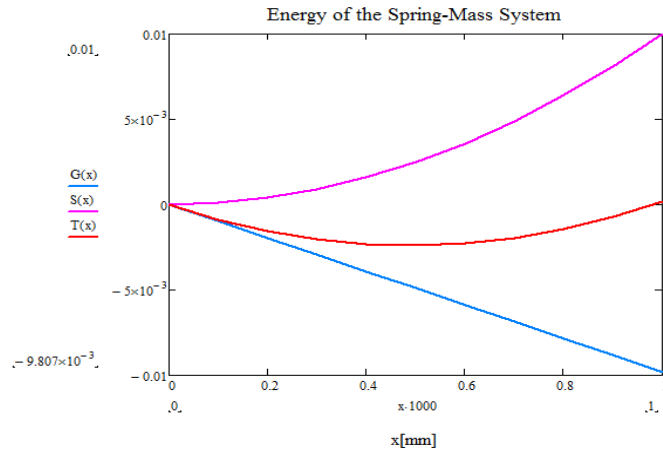


Figure 6. Energy as a function of x

It can be seen that a minimum of the total energy (red curve) is at $x^* = 0.4905\text{mm}$. Now let's consider the same spring mass system, however this time a rigid plane is introduced to establish a contact problem. *Figure 7* shows the configuration.

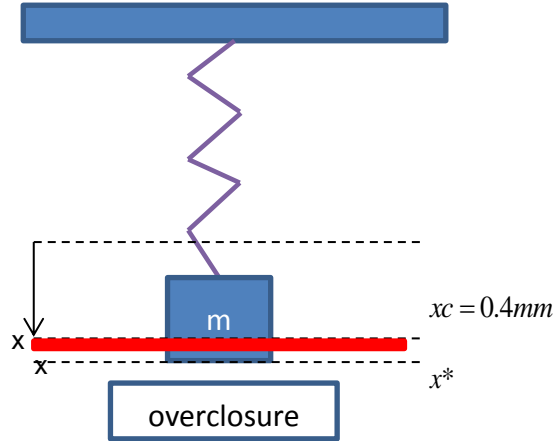


Figure 7. Spring mass system with rigid plane

In order to solve this contact problem the total energy equation will be turned into a constrained problem:

$$T(x) = G(x) + S(x) + \frac{1}{2} \epsilon p^2(x)$$

This is also called the penalty method, because it punishes overclosure, such as displayed in Figure 7, by adding energy to the system. ϵ is a constant and $p(x)$ a function of x :

$$p(x) = \langle x - xc \rangle$$

The brackets $\langle \rangle$ have been introduced by Macaulay and simply mean:

$$\langle x \rangle = \begin{cases} x, & \text{if } x \geq 0 \\ 0, & \text{otherwise} \end{cases}$$

For the current problem this results in the application of penalty energy only when overclosure is present. The corresponding energy graph is depicted in Figure 8.

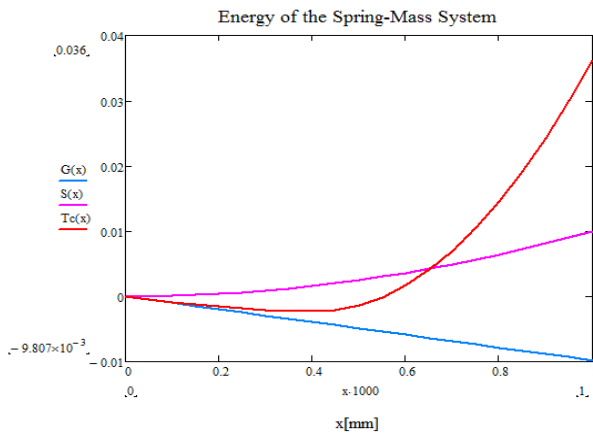


Figure 8. Energy as a function of x for the constrained problem

Again the solution is derived by calculating the first derivative of the total energy. The solution yields:

$$x^* \cong 0.41mm$$

Interestingly there is a difference between the solution and the position of the plane of 0.01 mm. This is due to the nature of the penalty method, which permits a small overclosure. However, by using a very high value for ϵ the error can be minimized.

This principle can also be applied to much more complex geometries by using the finite element method, as *Figure 9* shows. In this case a mesh size of about 1 μm is necessary to resolve the problem.

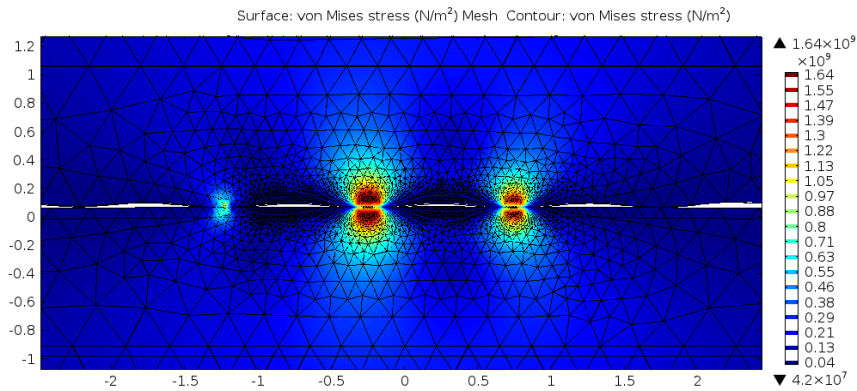


Figure 9. Finite element method applied on a contact problem

In this scenario a smooth surface and a rough surface are loaded against each other. High stress concentrations typically occur at the asperities. In this case the mises stress is evaluated. Numerical contact models come with several advantages:

- ◆ accurate modelling of real surfaces,
- ◆ consideration of non-linear material behaviour possible,
- ◆ inter-asperity interactions are considered,
- ◆ local stress evaluation.

However, the big disadvantage is the high numerical cost which is necessary for the resolution of contact problems. This results from the fact that the problem is highly non-linear because neither the contact area nor the contact stress are known a-priori.

5. CONCLUSION AND OUTLOOK

The importance of accurate modelling of mixed friction has been pointed out, whereby the focus has been laid on the functionality of different contact models. Statistical models can be used for straightforward modelling of contacts by using certain parameters of surfaces. They provide accurate results for moderate loadings

and are often used for modelling conforming contacts like journal bearings. However, limitations such as isolated asperity treatment or the lack of information of local stresses present drawbacks.

On the other hand a numerical method, which is based on the finite element method combined with the penalty method, has been presented. Surfaces can be modelled accurately and inter-asperity interactions are taken into account. Furthermore local stresses can be evaluated. The biggest drawback is the high computational cost, which is in the nature of this kind of methods. Both methods can be integrated into state of the art EHD solvers which have been presented in [3] and [4] in order to deepen the understanding of phenomena taking place in heavily loaded non-conforming machine elements.

6. ACKNOWLEDGMENT

Financial support by the Austrian Federal Government (in particular from Bundesministerium für Verkehr, Innovation und Technologie and Bundesministerium für Wissenschaft, Forschung und Wirtschaft) represented by Österreichische Forschungsförderungsgesellschaft mbH and the Styrian and the Tyrolean Provincial Government, represented by Steirische Wirtschaftsförderungsgesellschaft mbH and Standortagentur Tirol, within the framework of the COMET Funding Programme is gratefully acknowledged.

REFERENCES

- [1] ZUM GAHR, K.-H.: *Reibung und Verschleiß*. Wiley, 2004.
- [2] GREENWOOD, J.–WILLIAMSON, J.: Contact of Nominally Flat Surfaces. *Proceedings of the Royal Society*, 1966.
- [3] MODER, J.: *Mixed friction phenomena in non-conforming contacts*. Diplomarbeit. Montanuniversität Leoben, 2014
- [4] KRAMPL, H.: *Numerische und versuchstechnische Beurteilung geschmierter Kontakte inhomogener Werkstoffe*. Dissertation. Montanuniversität Leoben, 2012.

JOURNAL BEARING OPTIMIZATION FOR MINIMUM LUBRICANT VISCOSITY

FERENC JÁNOS SZABÓ

associate professor

*University of Miskolc, Institute of Machine and Product Design
3515 Miskolc-Egyetemváros
machszf@uni-miskolc.hu*

Abstract: In this paper the optimum geometry of journal bearings is determined for the minimum possible viscosity of the lubricant. During the investigations the basic equation of the THD (Thermo-hydrodynamic) state of hydrodynamic journal bearings is solved by using the finite difference technique, while for the optimization the RVA (Random Virus Algorithm) is used. Design variables are the coordinates of the 40 keypoints selected for creating the finite difference mesh. All the operational and geometry limits are included as implicit constraints. As the result of the optimization process, the lubricant viscosity can be considerably decreased compared to the starting design, this makes possible to apply water as lubricant in the bearing. This will decrease the lubricant cost by more than 95%, which is a very important achievement.

Keywords: *Journal bearing, minimum viscosity of lubricant, multidisciplinary optimization, evolutionary RVA algorithm*

1. INTRODUCTION

Thermo-hydrodynamic sliding and journal bearings are commonly used in many fields of mechanical and energy engineering. The lubricant is a very important component in these bearings. In many cases oil is used as lubricant, but nowadays one can find other materials too, used as lubricants (metals, water, air, gases, grease etc.). The most important characteristics of the lubricant in point of view of the operational parameters of the journal bearings is the viscosity. Oils and greases provide relatively high viscosity but they are expensive comparing to some smaller viscosity lubricants (water, gas, air) which could be cheaper. This thinking leads to application of the methods of Multidisciplinary Optimization (MDO) for journal bearing optimization with the lubricant viscosity as objective function to be minimized. If the necessary lubricant viscosity for the appropriate operation of the bearing can be decreased enough, this result can give the possibility to use smaller viscosity (and cheaper) lubricant, which will decrease considerably the lubricant costs. Changing the lubricant material from oil to air or water could be very useful from environmental protection point of view too. In some fields of life (agriculture, food industry, water plants or pumps, or for some other industrial applications)

water is very close or maybe it is a part of the working process so it will be easy to provide or in some cases it will be not so bad if some drops of the lubricant (water) will go into the processed material (in this case it must be clean enough) so the sealing could be simpler or cheaper too.

Finding the optimum geometry of journal bearings for minimum lubricant viscosity needs optimization techniques, while the effects of the temperature (THD state, Thermo-Hydrodynamic State) will enlarge the analysis process into a multiphysics or multidisciplinary analysis process. Therefore the whole optimization process will be an example of Multiphysics Optimization or Multidisciplinary Optimization (MDO). The disciplines involved in this complex process are: fluid flow, heat transfer, solid mechanics, elasticity and tribology. The complexity of these analysis processes makes it necessary to use several numerical methods (finite difference, finite element), which can sometimes be time consuming and takes a large amount of computing capacity. Therefore very efficient and quick optimization algorithms are needed for the Multidisciplinary Optimization of hydrodynamic bearings, in order to avoid overwhelming calculations and excessively long calculation times.

During the last 2-3 decades, evolutionary type optimization algorithms have provided the best ways to solve MDO problems, because of their efficiency, robustness and quick convergence. The basic idea of these algorithms came from the study of the behaviour and reproduction of several natural systems such as genetic engineering (Genetic Algorithm GA [2]), evolution of biological populations (Evolutionary Programming EP, or Evolutionary Strategies ES), Reproduction of Bacteria (Bacterial Foraging Algorithm, BFA), behaviour of natural swarms (Particle Swarm Optimization, PSO , or Virus-Evolutionary Particle Swarm Optimization VEPSO), behaviour of animal colonies (Ant Colony Algorithm, ACA), or behaviour and reproduction of viruses (evolutionary type Random Virus Algorithm, RVA [6]).

In this paper the Random Virus Algorithm (RVA) is used for the optimization of hydrodynamic journal bearings. For the numerical analysis of the hydrodynamic bearings in each step the finite difference technique is used. The temperature dependence of the lubricant characteristics (density, viscosity) is taken into consideration by iterative steps during the numerical solution of the governing partial differential equation. The objective function of the optimization is the lubricant viscosity needed for the appropriate operation and good load carrying capacity of the bearing. During the optimization the minimum of the objective function is sought.

As the result of the optimization the lubricant viscosity is decreased in a so great extent that instead of oil lubricant water can be used. This will decrease the lubricant costs by more than 95% and it can have very important environmental protection advantages, too.

As further development of this work, the multidisciplinary optimization of gear tooth geometry for higher safety against seizure will be investigated, applying the presented process.

2. SOLUTION OF THE THD STATE OF THE JOURNAL BEARINGS

The applied numerical method is applicable to any problem that can be described by linear partial differential equations. In this work it is used for solving the pressure distribution $p(x,z)$ in the fluid film of hydrodynamic journal bearings, for a given gap shape function $h(x,z)$. The governing equation of this problem is the Reynolds-equation:

$$\frac{\partial}{\partial x} \left(h^3 \frac{\partial p}{\partial x} \right) + \frac{\partial}{\partial z} \left(h^3 \frac{\partial p}{\partial z} \right) - 6\eta U \frac{\partial h}{\partial x} - 12\eta \frac{\partial h}{\partial t} = 0 \quad (1)$$

In *Equation (1)* the relative velocity of the sliding surfaces is denoted by U , and η means the absolute viscosity of the lubricant.

Equation (1) can be written into matrix form, after the discretization of the fluid film domain between the sliding surfaces, by using finite differences, as shown in *Equation (2)*. The vector p collects the nodal values of the pressure function, and elements of matrix K depend on the nodal values of the gap shape function:

$$Kp + g = 0 \quad (2)$$

In case of a finite difference mesh having $u \times v$ nodes, the matrix K will have a bandwidth of $2v-3$, after the applications of the boundary conditions.

The density and the viscosity of the lubricant is the function of the operating temperature of the bearing. This is taken into account by an iteration during this numerical solution. At the beginning, an approximate temperature is supposed and the equation is solved with characteristics calculated for this temperature. On the basis of the results, new and more accurate temperature value can be determined. The whole calculation will be repeated with lubricant characteristics calculated with this new temperature value. Several trial-calculations and experiences show that after three or four iteration cycles the difference between the temperature values before and after a calculation step will be smaller than 1 °C, which is enough accurate for the further calculations. The elastic deformation of the shaft and housing could be checked by finite element model after the solution (quasi-TEHD state), this could be effective if these deformations are small comparing to the gap size (for example in case of steel shaft and steel bushing).

Once we have the solution of this process for the nodal values of the pressure function, the load carrying capacity of the surface pairs F_n can be calculated by numerical integration, using the characteristic sizes (r, R, b, h_o, e) of the bearing.

$$F_2 = \int_{\varphi=-(\beta-\varphi_1)}^{\varphi_1} \int_{z=-\frac{b}{2}}^{b/2} p r d\varphi dz \sin \varphi \quad F_1 = \int_{\varphi=-(\beta-\varphi_1)}^{\varphi_1} \int_{z=-\frac{b}{2}}^{b/2} p r d\varphi dz \cos \varphi$$

$$F_n = \sqrt{F_1^2 + F_2^2} \quad (3)$$

The friction force, which is the force needed for the relative motion between the shaft and bushing can be determined as follows:

$$F_f = \int_{x=-r(\beta-\varphi_1)}^{r\varphi_1} \int_{z=-\frac{b}{2}}^{b/2} \left(\frac{1}{2} \frac{\partial p}{\partial x} h - \eta \frac{r\omega}{h} \right) dx dz \quad (4)$$

In *Equation (4)* the angular velocity $\omega = 2 \Pi n$, if the unit of the angular velocity is radians per seconds and the n rotation speed is in rotations per seconds. The frictional coefficient μ can be calculated as $\mu = F_f / F_n$. Lubrication angle β together with the angle φ mark a general position of the gap function $h(\varphi)$.

$$h(\varphi) = R - r - e \cos \varphi \quad (5)$$

This calculation method has been verified and compared to the analytical solutions for infinite width bearings given by SZOTA and DÖBRÖCZÖNI [3], optimized for maximum load carrying capacity, and good agreement was found between the theoretical and numerical results [5]. Another verification of the method was in the case of finite sliding bearings [4], [5] where the results of this finite difference based code were compared with those calculated by the ANSYS-FLUENT [1] program system and once again good agreement was detected.

3. THE RVA OPTIMIZATION ALGORITHM

The design variables are the nodal coordinates of the finite difference mesh keypoints. For the meshing 40 key nodes are used with variable coordinates (these are the optimization variables) and remaining nodes are placed depending on the keypoints in order to make higher density mesh. For the optimization problem presented here the objective function is the lubricant viscosity η which is to be minimized. Size constraints: $0 \text{ [mm]} < r < 500 \text{ [mm]}$, $0 \text{ [mm]} < R < 500 \text{ [mm]}$, $0 \text{ [mm]} < e < 10 \text{ [mm]}$. Implicit constraints: the pressure function should fulfil the Reynolds equation (1) of hydrodynamic surface pairs; the shaft diameter should be higher than the minimum required diameter given in *Equation (6)*; the average pressure in the fluid film should be smaller than the maximum permissible average pressure (2 MPa) as it is shown in *Equation (6)*; and the minimum gap distance h_0 should be higher than the sum of the maximum roughness of the surfaces plus the elastic deformations of the surfaces. Maximum permissible operational temperature is 80 °C for oil and 40 °C for other lubricant (e.g. water).

$$r \geq 0.5 \sqrt{\frac{F}{\bar{p}_{adm} b/d}} \quad h_0 \geq 4.5(R_{a1} + R_{a2}) \quad \bar{p} \leq \bar{p}_{adm} \quad (6)$$

According to the logic of the RVA optimization algorithm, the first step is to create the first (or starting) population of the possible solutions fulfilling the constraints.

Once the starting population has been generated, each member of the population will reproduce, creating three new members each. This process is stronger than a nuclear explosion, so in the remaining part of the optimization the selection of the best members and elimination of members without good enough objective function values will be very important. At least 60% of the new and of the total members should be eliminated after each population in order to avoid overwhelming calculations. The members that survive this strict selection procedure will give the second population. The programming of the RVA algorithm is very simple, easy to carry out in any programming language or in macro languages of finite element program systems, if available.

This procedure will continue until the pre-defined optimum conditions are fulfilled. Several benchmark problem runs and numerical experiments have shown that the algorithm is very efficient: in the optimization problem investigated in this work 5 populations were enough to find the optimum. The total computation time required for a complete run was 23 minutes on an Intel core i5 desktop computer. The j th population: $P_j = \{x_i\}_j$; the reproduction formula:

$$y_k = x_k + R_k q^* (up_i - lw_i) \quad (7)$$

Where y_k means the k^{th} variable value of the new member, q^* is the spreading parameter, and R_k is a random number between 0 and 1, simulating the possibility of random mutations. Setting the spreading parameter properly is also very important, because it can have a considerable effect on the efficiency of the algorithm. This needs a great deal of experimentation and unique fine-tuning work for each optimization problem. For this optimization process the best value for the spreading parameter was 0.65 in the first three populations and 0.29 afterwards.

If the maximum number of iterations is reached without fulfilling the convergence criteria, it means that the search procedure needs more iterations and so the optimization is stopped, but during the results display a warning will say that there is a danger of a local optimum and possibly a new run will be necessary with other parameters or with a higher maximum number of iterations permitted.

4. RESULTS OF THE OPTIMIZATION

As numerical example a hydrodynamic journal bearing of an electric generator has been optimized by using the multidisciplinary optimization (MDO) procedure described in the *Section 2* and *3*.

Table 1 shows all the important parameters of the bearing, after calculating the most important sizes of the bearing from the optimal design variables. In the table it can be seen that important achievement was made in the objective function value as results of the optimization:

Table 1
Optimization results for two different objective functions

	r [mm]	R [mm]	e [mm]	μ	F_n [N]	T [°C]	\bar{p} [MPa]	Decr. in η [%]	h_o [μm]	Joint (ISO)
Starting	80	80,13	0,079	0,003	31400	74,9	0,943	–	50,54	H7/a9
Min. η	65	65,05	0,050	0,0006	31400	29,6	1,43	40	20,42	H7/a9

5. CONCLUSION

THD state journal bearings are optimized for minimum necessary lubricant viscosity. The design variables are the keynodes selected for the finite difference mesh during the numerical solution of the Reynolds-equation. The dependence of the lubricant characteristics from the temperature is taken into consideration by an iteration for the operation temperature.

For the optimization the RVA evolutionary type optimization algorithm was applied and the optimization process can be treated as Multidisciplinary Optimization example.

The most important achievement of the optimization is that the lubrication material of the bearing can be decreased from oil to water. This could decrease the lubricant cost by more than 95% and can provide important environmental protection advantages.

Using the *Table 1* designers and users of the bearings can find how to redesign the bearing in order to realize the water lubrication state having all the most important operational characteristics of the bearing (load carrying capacity and friction coefficient) remain the same or slightly improved.

Further investigations will be made for the optimization of gear tooth for minimum danger of seizure.

6. ACKNOWLEDGEMENTS

The research work presented in this paper is based on the results achieved within the project TÁMOP 4.2.1.B-10/2/KONV-2010-0001 in the framework of the New Hungarian Széchenyi Plan. The realization of this project is supported by the European Union and co-financed by the European Social Fund.

REFERENCES

- [1] ANSYS Inc.; SAS IP Inc.: *ANSYS Mechanical APDL Technology Demonstration Guide*, Southpointe, 275 Technology Drive, Canonsburg, PA 15137, USA, 2011.
- [2] GOLDBERG, D. E.: *Genetic Algorithms in Search, Optimization and Machine Learning*. Addison-Wesley, Massachusetts, USA, 1989.

-
- [3] SZOTA, Gy.–DÖBRÖCZÖNI, Á.: Influence of the adhesiveness of lubricants on load carrying capacity and coefficient of friction of hydrodynamic sliding surface pairs. In: STACHOWIAK, G. W. (ed.): *AUSTRIB'94 International Tribology Conference*. Perth, Australia, 5–8 December, 1994, 135–139.
 - [4] KOVÁCS, B.–SZABÓ, F. J.–SZOTA, Gy.: A generalized shape optimization procedure for the solution of linear partial differential equations with application to multidisciplinary optimization. *Structural and Multidisciplinary Optimization*, 21, No. 4 (2001), 327–331.
 - [5] SZABÓ, F. J.: Edge Shape Optimization of Finite Width Sliding Bearings. *Comput. Sci. Appl.*, Vol. 2, No. 1 (2015), 29–35.
 - [6] SZABÓ, F. J.: Multidisciplinary optimization of a structure with temperature dependent material characteristics, subjected to impact loading. *International Review of Mechanical Engineering*, Vol. 2, No. 3 (2008), 499–505.

THEORETICAL VIBRATION ANALYSIS OF A MANUFACTURING DEVICE

ATTILA SZILÁGYI–GYÖRGY TAKÁCS–DÁNIEL KISS–DÁNIEL TÓTH

*University of Miskolc, Department of Machine Tools
3515 Miskolc-Egyetemváros
szilagyi.attila@uni-miskolc.hu;
takacs.gyorgy@uni-miskolc.hu;
kiss.daniel@uni-miskolc.hu;
toth.daniel@uni-miskolc.hu*

Abstract: This article explores a certain theoretical method for investigating a large-sized manufacturing device for face-milling rectangular aluminium ingots. First a single DOF (degree of freedom) dynamic model which contains a piecewise linear spring force and damping is created, then the governing equation system is established which is solved by the means of numerical analysis. As a consequence, the theoretically obtained results are compared to the ones gained by the experimental investigations.

Keywords: *analytical dynamics, nonlinear vibration, numerical methods*

1. INTRODUCTION

A theoretical investigation of a large-sized face-milling device is detailed in this article. This machine is applied for the improvement of the surface quality of aluminium ingots manufactured by face-milling. This operation is required by the high demands made on the multi-layered rolled aluminium products from the side of the automotive industry. The remanent surface roughness however, as the result of the face-milling process, often brings forth problems in the forms of bubbles, inclusions during the subsequent multilayered rolling procedure. To eliminate this problem, several technological experiments, investigations and modifications had been carried out and implemented, the surface roughness of the ingots, however, still have not been approved enough, and not always met the requirements. In summary, some 50% improvement of the surface quality had been achieved as the result of the technological investigations.

Besides these improvements, which still have turned out to be unsatisfactory in several cases, investigations have revealed additional concerns. The theoretical surface roughness for example, which comes purely from the geometry of the cutting inserts, the feedrate and the depth of cut, still has not been able to be achieved, hence some other sources of the surface errors need to be searched for, which might come from the dynamic properties of the manufacturing device.

The face-milling device and the aluminium ingot are depicted in *Figure 1*, and clearly seen that a portal-type milling machine is investigated. Face-milling of the aluminium ingot (*1*) is performed by the milling disk (*2*), and the feeding motion is perpendicular to the drawing plane and takes place between the columns.

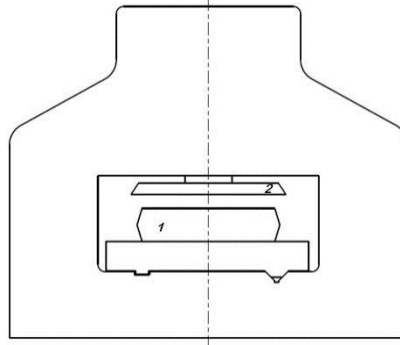


Figure 1. The portal-type face-milling machine

2. THE OBJECTIVE AND THE METHOD OF THE THEORETICAL INVESTIGATIONS

The main objective of the investigations on one hand is to reveal the dynamic properties of the milling machine, focusing on the possible sources of vibration which might affect the surface quality and, on the other hand, the validation of the experimental results obtained by the instrumental vibration analysis.

First of all the 1-DOF vibroimpact-type dynamic model of the device is created, then the piecewise linear governing equations are established which then are solved with the means of numerical analysis (R-K 4th-order) and, finally, the analytical results are compared to the profilograms displaying the surface roughness of the ingot and had been recorded after the face-milling process.

3. THEORETICAL ANALYSIS

A single-DOF, periodically excited vibro-impact model is considered, which contains some additional features, such as a gap of y_0 , a mass point of m , and a piecewise linear spring [1] and dampings. This model is based on some results of a former experimental investigation where the gap of $y_0 = 0,4 \text{ mm}$ had been detected within the ball bearings and which is assumed to be the source of the axial vibration of the spindle-milling disk assembly. Due to our assumption, this gap might play an important role in the inappropriate surface roughness of the ingot. This article is supposed to demonstrate our “a priori” assumption.

3.1. The dynamic model

During the face-milling procedure, the axis of the spindle – milling-disk unit is bevelled to the face of the ingot to be manufactured in order to avoid the

manufactured surface from the returning cutting edges. As a result of this bevelled position is seen in *Figure 2*, and, since the stiffness of the milling-disk is much less than that of the spindle and acts like a spring, the cutting edges, due to the stimulation of the cutting procedure, will perform vibrations which influences the expected theoretical surface roughness by making it more irregular and, in some cases, unacceptably wavy. This suggests that the insufficient stiffness of the milling-disk and the axial gap within the rolling bearings which induce the axial vibration of the spindle unit, are of great importance in respect with the irregular surface quality of the ingot. This theoretical assumption is going to be demonstrated in the followings. The dynamic model applied for the investigations is depicted in *Figure 2*.

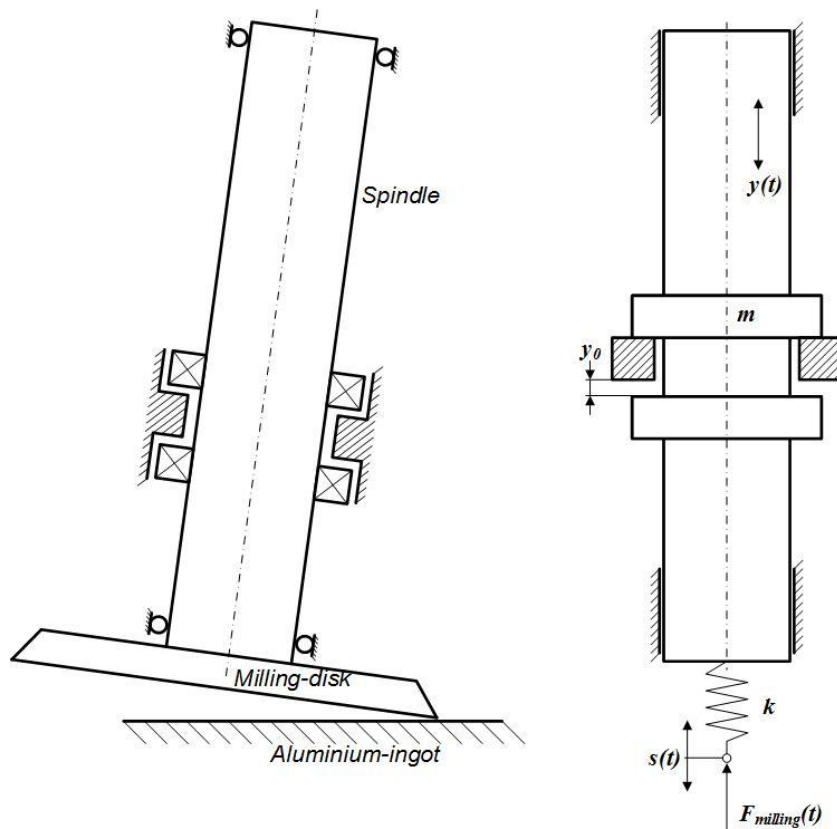


Figure 2. The dynamic model of the spindle – milling-disk assembly

During the analysis the spindle is assumed to be a rigid body with the mass of m , while the milling-disk is considered to be a massless spring having the stiffness of k and which is connected to the spindle at one end, and periodically excited by the cutting procedure ($F_{milling}(t)$) at the other end. The vibration is assumed to be

uniaxial, and performed along only the Y -axis, and the maximal displacement of the mass is y_0 .

Two different types of damping are considered during the analysis: the material damping on one hand, which is acting when the spindle impacts into the walls of the gap and, on the other hand, the Coulomb-type damping, which comes from the friction between the sliding parts.

3.2. The mass and the spring elements of the model

The main conclusion of this investigation is the displacement of the point of the cutting edge in cut vs. time, which function enables us to draw another conclusion on the surface quality of the ingot. The considered point is the acting point of the stimulating force coming from the cutting procedure. The numerical values of the above mentioned parameters had been established by the former technological experiments, the drawing documents from the side of the company, and by estimations based on the literature. First of all the 3D assembly model of the spindle – milling-disk unit (*Figure 3*) was created by which the mass of the entire unit could be calculated yielding $m = 6000 \text{ kg}$.



Figure 3. The 3D CAD model of the spindle – milling-disk assembly

The total weight of the mass point of the dynamic model (*Figure 2*, m) comes from the sum of the masses of the spindle and the milling-disk, hence the mass of the „spring” in the model shall be neglected in the followings. By the 3D model seen in *Figure 3* the stiffness k of the milling-disk, which is the spring constant of the model (*Figure 2*, k), has also been calculated by FEM (*Figure 4*). By the slope of the diagram, the stiffness of the spring is $k \approx 5 \cdot 10^8 \frac{\text{N}}{\text{m}}$.

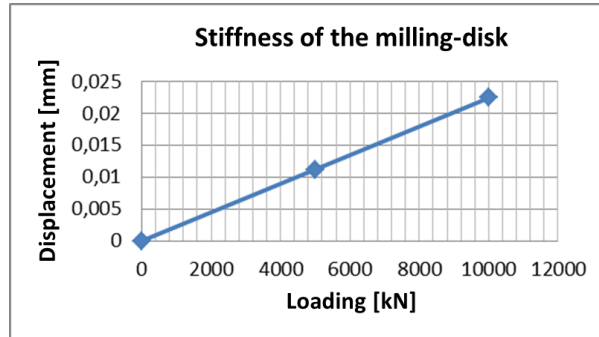


Figure 4. The stiffness (force vs. displacement) curve of the spring-like milling-disk

3.3. The stimulating force

This force is assumed to be periodic and this chapter is exploring a method for establishing the stimulating force vs. time. See *Figure 5* which depicts the geometrical and kinematical conditions of the milling-disk and the ingot at a certain time of the manufacturing process. B , D , n and z are the width of the ingot, the diameter, rotational speed and the number of the cutting edges of the milling disk respectively. Due to the cutting edges cut into the material one after the other, and each cut will act as an impulse-like stimulation the axial component of the cutting force is considered to be periodical.

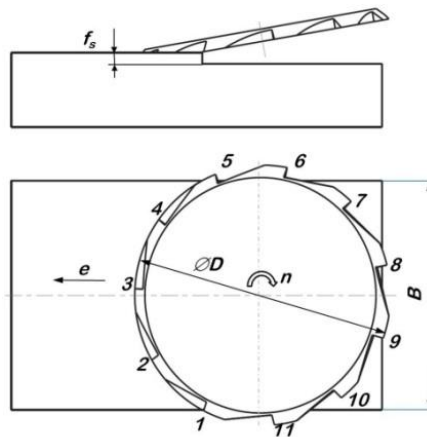


Figure 5. The milling-disk and the ingot

Using the above mentioned parameters, simple expressions can be set up to calculate the rotational time T of the disk, the time τ which is spent in cut by each edge and the time interval ΔT which takes between two neighbouring edges get into cut. In order to be able to establish the expression of the cutting force vs. time, the following numerical values are taken into consideration: $B = 1850 \text{ mm}$,

$D = 2100 \text{ mm}$, $n = 530 \text{ 1/min}$, $z = 11$, by which the unknown time intervals yields

$$T = \frac{60}{n}, \quad \tau = \frac{T}{\pi} \arcsin\left(\frac{B}{D}\right), \quad \Delta T = \frac{T}{z}.$$

As regards the axial component of the cutting force, which the edges are exposed to, the followings are considered:

- The position is illustrated in *Figure 5* is assumed to be the $t=0$ initial position, where the cutting edge 1 is about to start to cut the ingot, while the edges 2, 3 and 4 are already in cut;
- The absolute value of the axial component acting on the edges in cut is assumed to be constant while the edge is cutting, $F_0 = 6,5 \text{ kN}$ [2].

As an example, the axial component of the cutting force acting on edge 2 vs. time is seen in *Figure 6*.

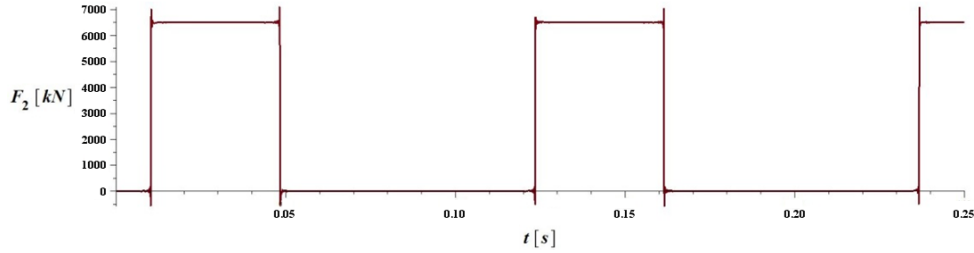


Figure 6. The axial cutting force acting on edge 2 vs. time

As it can be seen in *Figure 6*, the assumed shape of the axial force component acting on each edge in cut is rectangular with the length of τ , height of F_0 and, which is repeated by T . Due to the discontinuity, both the analytical and numerical investigation of this expression is difficult, so the application of the Fourier-series seems to be a reasonable way to overcome the problems of discontinuity. The general finite (including N members) form of the Fourier-series of the axial cutting force acting on the edge i can be written in the form of

$$\tilde{F}_i = F_0 \left\{ \frac{\tau}{T} + 2 \sum_{n=1}^N \left[\frac{1}{n\pi} \sin\left(\frac{n\pi\tau}{T}\right) \cos\left(\frac{2n\pi}{T} \left(t - \frac{\tau}{2} - (i-1)\Delta t\right)\right) \right] \right\} \quad (1.1.)$$

[3]. Summarizing all the \tilde{F}_i components, the total force $F_{\text{milling}}(t) = \sum_{i=1}^{11} \tilde{F}_i(t)$ acting

on the milling-disk during manufacturing is obtained. The curve vs. time can be seen in *Figure 7*, where $N = 200$ members of the Fourier-series are taken into consideration. Since there are 4 cutting edges in cut at the same time, the amplitude of the assumed cutting force is 26 kN .

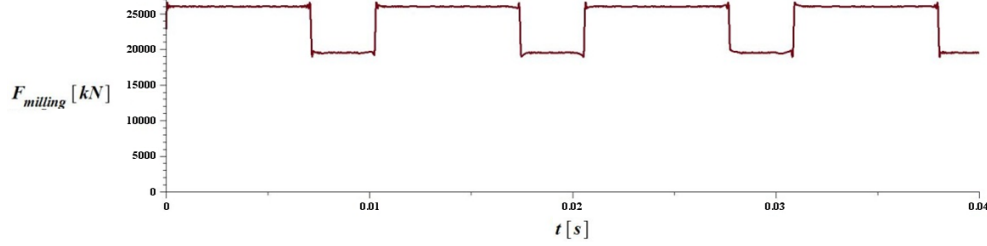


Figure 7. Periodical stimulating force approximated by Fourier-series

As it is mentioned above, besides the material damping, which is assumed to be linear, a piecewise linear damping from the Coulomb-friction is also contained by the dynamic model. The Lehr-type coefficient of the linear material damping is assumed to be $\varrho = 0,0002$ [4]. The absolute value of the Coulomb-force can be estimated by the reaction forces acting at the supports of the main spindle, and can be calculated by setting up the necessary static equations, which are not detailed below. During the analysis, the dynamic coefficient of friction is assumed to be $\mu_d = 0,03$ [5] which multiplied by the sum of the radial components of the reaction forces, then yields the absolute value of the friction force, $S = 300 \text{ N}$, and which originally comes from the axial relative slip of the main spindle and the rolling element bearings. Thus the Coulomb-type friction is considered in the form of $F_s = S \cdot \text{sgn}(\dot{y})$, where sgn denotes the signum-function.

Hence, the

$$\dot{y} = z$$

$$\dot{z} = -\frac{1}{m} \left\{ \frac{2\varrho}{\sqrt{km}} \dot{y} + F_s \text{sgn}(\dot{y}) + ky + \frac{1}{2} k' (|y - y_0| - |y + y_0|) + k'y + mg - F_{\text{mar}\acute{o}}(t) \right\} \quad (1.2.)$$

governing equations of the dynamic model seen in Figure 2 can be set up, where the quantity

$$s(t) = \frac{1}{k} \left[m\dot{z} + \frac{2\varrho}{\sqrt{km}} \dot{y} + F_s \text{sgn}(\dot{y}) + ky + \frac{1}{2} k' (|y - y_0| - |y + y_0|) + k'y + mg \right] \quad (1.3.)$$

provides the approximate axial displacement of the edges currently in cut. For the numerical solution of (1.2.) the following parameter values are assumed: the total mass of the spindle and the milling-disk $m = 6000 \text{ kg}$, $k = 5 \cdot 10^8 \frac{\text{N}}{\text{m}}$ the stiffness of the milling-disk which is regarded as a linear spring, the axial gap within the bearings $y_0 = 0,4 \text{ mm}$, and $k' = 5 \cdot 10^{12} \frac{\text{N}}{\text{m}}$ the stiffness of the edges which imitate the gap, and whose stiffness is assumed to be 4-order higher than that of the linear spring. Additional assumption is that $y = 0$ is the midpoint of the y_0 gap, thus the maximal displacement of m is $\pm 0,2 \text{ mm}$. The initial conditions are set up as

follows: $t = 0$, $y(0) = -0,2 \text{ mm}$, $\dot{y}(0) = 0$, i.e the spindle is “seated” on the gap when manufacturing about to start.

The numerical solution is obtained with the application of MAPLE 12. Due to some numerical pre-experiments, it was revealed, that from $t = 10 \text{ s}$ the vibration becomes stationary, thus the investigations are ranged by the time interval of $t \in [10, 11] \text{ s}$ (Figure 8).

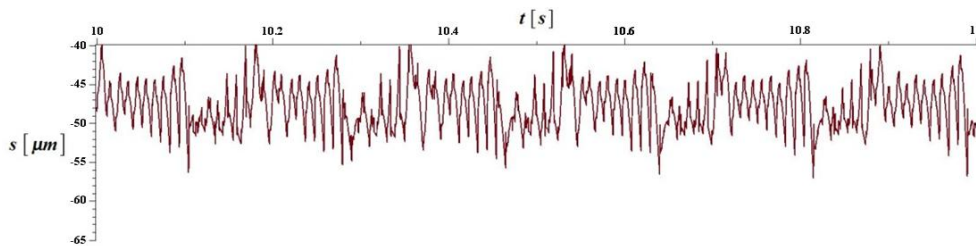


Figure 8. The axial displacement of the cutting edges in cut during the manufacturing

It is clearly seen in Figure 8 that the cutting edges will perform a modulated vibration, which is very similar to the profilogram recorded over the manufactured surface of the ingot (Figure 9).

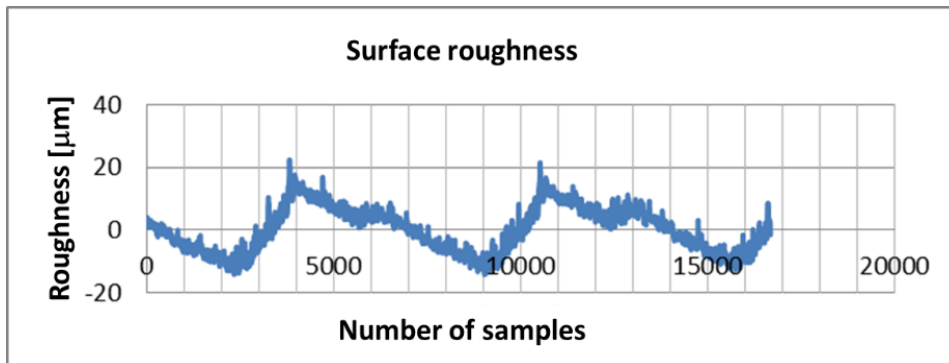


Figure 9. Profilogram registered during the surface roughness detection

It is also visible in Figure 8, that the maximum depth of the vibration is roughly $20 \mu\text{m}$, and which is less than that of the profilogram, $30 \mu\text{m}$. The difference might come from the ignorance of some other vibration source, which also active and, even amplified during manufacturing. In spite of this slight difference, the 1 DOF dynamic model provides a very good approximation about one of the main sources of vibration and a good reproduction of the pictogram obtained by the surface roughness measurement of the ingot.

4. SUMMARY

A theoretical investigation of a large-sized manufacturing device is detailed in this article by the means theoretical dynamics and numerical analysis. A 1 DOF dynamic model was created, then the piecewise linear governing equations were set up and, finally, the numerical solution of this equation system was obtained. As a consequence, a good correlation can be seen between the theoretical and the a priori experimental results.

5. ACKNOWLEDGEMENT

This research was carried out as part of the TÁMOP-4.2.1.B-10/2/KONV-2010-0001 project with support by the European Union, co-financed by the European Social Fund, in the framework of the Centre of Excellence of Mechatronics and Logistics at the University of Miskolc.

REFERENCES

- [1] SHAW, S. W.–HOLMES, J. P.: A periodically forced piecewise linear oscillator. *Journal of Sound and Vibration*, Vol. 90, No. 1 (1983), 129–155.
- [2] *Tuskómaró forgácsolási paramétereinek fejlesztése*. Kutatási jelentés, 2009. 10. 07.
- [3] FODOR, Gy.: *A Laplace-transzformáció műszaki alkalmazása*. Műszaki Könyvkiadó, Budapest, 1966.
- [4] MAKHULT, M.: *Gépalapok rezgéstani méretezése*. KGM Műszaki Tájékoztató és Propaganda Intézet, Budapest, 1962.
- [5] MOLNÁR, L.: *Szerszámgépek vezetékei I. Csúszóvezetékek vizsgálata tribológiai rendszerszemléletben*. Oktatási segédlet, Miskolc, 1988.

REVIEWING COMMITTEE

Á. DÖBRÖCZÖNI	Institute of Machine and Product Design University of Miskolc H-3515 Miskolc-Egyetemváros, Hungary machda@uni-miskolc.hu
M. GERGELY	Acceleration Bt. mihaly_gergely@freemail.hu
K. JÁRMAI	Institute of Materials Handling and Logistics University of Miskolc H-3515 Miskolc-Egyetemváros, Hungary altjar@uni-miskolc.hu
I. KERÉKES	Institute of Mechanics University of Miskolc H-3515 Miskolc-Egyetemváros, Hungary mechker@uni-miskolc.hu
F. J. SZABÓ	Institute of Machine- and Product Design University of Miskolc H-3515 Miskolc-Egyetemváros, Hungary machszf@uni-miskolc.hu
A. SZILÁGYI	Department of Machine Tools University of Miskolc H-3515 Miskolc-Egyetemváros, Hungary szilagyi.attila@uni-miskolc.hu
J. PÉTER	Institute of Machine and Product Design University of Miskolc H-3515 Miskolc-Egyetemváros, Hungary machpj@uni-miskolc.hu

Secretariat of the Vice-Rector for Research and International Relations
University of Miskolc
Responsible for the Publication: Prof. Dr. Tamás Kékesi
Published by the Miskolc University Press under leadership of Attila Szendi
Responsible for duplication: Erzsébet Pásztor
Editor: Dr. Ágnes Takács
Technical editor: Csilla Gramantik
Corrector: Krisztina Mátrai
Number of copies printed: 50
Put the Press in 2016
Number of permission: TNRT-2016-400-ME
HU ISSN 1785-6892 in print
HU ISSN 2064-7522 online